Spring 2017

Lithospheric Evaluation of the Mid-Continental Rift System in Iowa from a Gravity and Magnetic Analysis

Moamen Mohamed Almaz
Missouri State University, almaz012@live.missouristate.edu

LITHOSPHERIC EVALUATION OF THE MID-CONTINENTAL RIFT SYSTEM IN IOWA FROM A GRAVITY AND MAGNETIC ANALYSIS

A Master's Thesis

Presented to

The Graduate College of

Missouri State University

In Partial Fulfillment

Of the Requirements for the Degree

Master Science, Geospatial Science in Geography, Geology and Planning

By

Moamen M. Almaz

May 2017

LITHOSPHERIC EVALUATION OF THE MID-CONTINENTAL RIFT SYSTEM IN IOWA FROM A GRAVITY AND MAGNETIC ANALYSIS

Geography, Geology and Planning

Missouri State University, May 2017

Master of Science

Moamen M. Almaz

ABSTRACT

The Proterozoic Midcontinent Rift System (MCRS) is considered one of the most important tectonic features in North America and was formed during a continental breakup event at 1.1 Ga (billion years). The MCRS is totally covered by Phanerozoic sedimentary rocks except in the Lake Superior region. Consequently, the geological characteristics of the MCRS are primarily inferred from extrapolations from the outcrop areas, drill holes, and from a variety of geophysical investigations. Iowa has a large segment of the MCRS which to date has only been partially investigated geophysically with little information regarding the lower crustal and upper mantle structure under the rift. Gravity and magnetic data were analyzed where Bouguer gravity, total-intensity magnetic and residual gravity anomaly maps clearly outline the main rift system with maxima anomalies over the basalt and minima anomalies over the flanking rift basins. Four gravity and magnetic models, perpendicular to the MCRS were constructed. These two-dimensional models are constrained by previous gravity and magnetic models performed elsewhere on the MCRS, seismic reflection data, basement penetrating drillholes and broadband seismic models. Even though the models are nonunique, they support the presence of lower crustal underplating materials formed by the extrusion of large amounts of mafic material from the upper mantle. These underplating materials are related to the plume derived magma. These deep roots mafic intrusions help resolving the controversy about the nature of the well-defined anomalies present in the area.

KEYWORDS: MCRS, Iowa, gravity, magnetic, models, underplating materials.

This abstract is approved as to form and content

_____

Dr. Kevin L. Mickus
Chairperson, Advisory Committee
Missouri State University

LITHOSPHERIC EVALUATION OF THE MID-CONTINENTAL RIFT SYSTEM IN IOWA FROM A GRAVITY AND MAGNETIC ANALYSIS

By

Moamen M. Almaz

A Master's Thesis
Submitted to the Graduate College
Of Missouri State University
In Partial Fulfillment of the Requirements
For the Degree of Master of Science, Geospatial Science
in Geography, Geology and Planning

May 2017

Approved:

_____
Dr. Kevin L. Mickus

_____
Dr. Melida Gutiérrez

_____
Dr. Xian Miao

_____
Julie Masterson, Dr: Dean, Graduate College

ACKNOWLEDGEMENTS

At first, I would like to thank God for everything. Then, thanks to the graduate college and my committee members Dr. Kevin Mickus, Dr. Melida Gutierrez and Dr. Xian Miao. I am heartily thankful to Dr. Kevin Mickus, my primary advisor, for encouragement, guidance and support from the first moment till now. He enabled me to expand my knowledge and understand how the research looks like. He was always available, and he supported me in several ways. He provides me by data, softwares, and advices. Thousands Tons of appreciation is extended to Dr. Melida Gutierrez, her help really can't be described. She is one of the best and fewest real professors I have dealt with. She is simply and deeply explain her classes. Thanks Dr. Melida from the moment I came here till the last day in my life.

The words can't express my thanks for my parents, Mohamed Almaz and Hoda Elsayed, may Allah bless them. They gave everything to me, the environment was really comfortable at home to study. I hope that I will be able to make them happy during my entire life. I really thank my brothers, Mostafa and Mahmoud, my friends, my family, my students in university, my small village, and my professors at MSU who helped me a lot, Dr. Gouzie, Dr. Michelfelder and my colleges who helped me a lot too, especially at the beginning, Ahmed Salem, Murat, Dexuan, Joe, Wes, Wes Weichert, Grant, Ben. Finally, I offer my regards to all of those who supported me in any respect for the period of the completion of the thesis and when I was back there in Egypt, all my professors Dr. Ziko, Dr. Khaled Saed, Dr. Attwa, Dr. Amin, Dr. Ahmed Saed, Ahmed Mansour and Attia.

Then, I want to dedicate this thesis to one of the greatest professors who has just passed away on December 6, 2016, Dr. Abdelmohsen Ziko. He was inspiring me from the first year I met him. He was encouraging me until I got a teaching assistant position in my college in Egypt. He was a real famous and humble professor. Whatever I could do for him, will not equal anything of what he has done for me. I was waiting to tell him that I got my master degree from America and I really wanted to see his eyes happy but he passed away. May Allah bless you Dr. Ziko. Rest in peace Dr. Ziko.

TABLE OF CONTENTS

LIST OF TABLES

LIST OF FIGURES

INTRODUCTION

1.1. Introduction

The mid-continental rift system (MCRS) or Keweenawan Rift system is one of the most well-known rifts around the world, it is considered a rift because of its morphology (Stein et al., 2015) of three large-scale arm components: the western arm; the Lake Superior arm; and the eastern arm, merging at Lake Superior (Fig. 1).

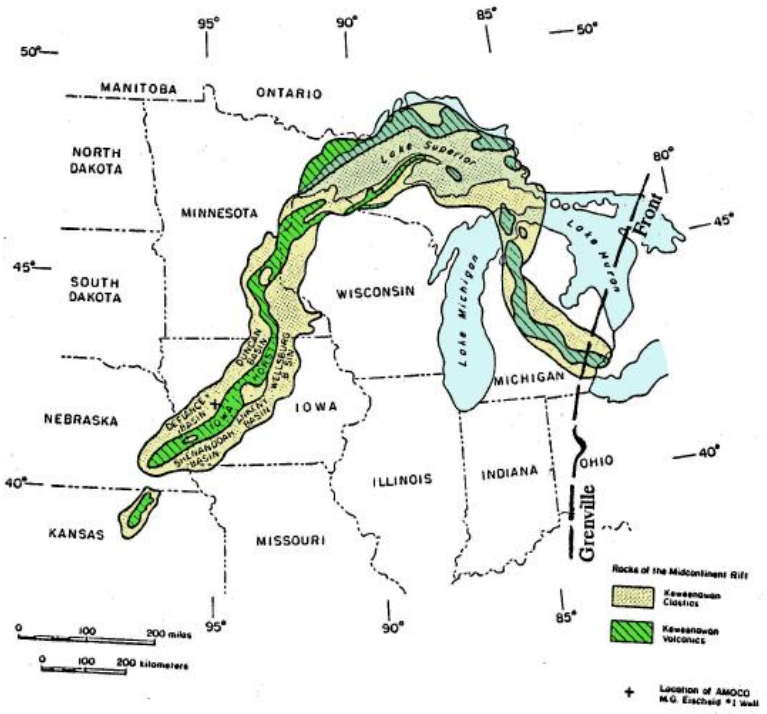

Figure 1. The location of the Midcontinental Rift system in the United States (Anderson, 1992).

The MCRS constitutes a great plateau basalt province, covering 100,000 km^2 and involving 1 x 10^6 km^3 of intrusive rocks (Green, 1982; 1989). Most of the MCRS is

covered by Phanerozoic sediments especially the western arm (Hinze et al., 1997) except the exposed areas in Lake Superior region of Minnesota, Wisconsin, and Michigan. The MCRS produces a prominent gravity anomaly in the central U.S. that reflects major geological features, and represents a significant episode in the history of the North American continental lithosphere (Van Schmus and Hinze, 1985). The gravity anomaly has higher values along the axial horst composed of mafic and plutonic rocks, which is surrounded by sedimentary basins indicated by the gravity minima.

Halls (1978) stated that the MCRS at the Lake Superior exposed belt, was formed initially be a period of tensile stress that led to volcanism, axial graben development, and the formation of a deep, clastic filled basin. This was followed by a compressional stress period that reversed the movement along the graben-bounding faults and forced the axial grabens upward through the overlying clastics leaving a central horst/flanking clastic-filled basin configuration (Anderson, 1992). The MCRS has been studied since 1800, by deep seismic reflection profiles, gravity, magnetic and few well logs. We used all these previous works to construct our model.

1.2. Purpose and Scope of Work

The purpose of this study is to examine the general crustal and upper mantle structure of the mid-continental rift system in Iowa (MCRS) through the analysis of gravity and magnetic data. We collected all the available data to use as constrains to build a model with the best possible solution out of the infinite number of solutions possible.

A series of gravity maps were created to qualitatively describe the general tectonic features of the MCRS, these included Bouguer gravity maps, tilt derivative

maps, and bandpass filtered maps. To get more quantitative details about the lithospheric structures, eight models along four cross-sectional profiles A-A', B-B', C-C', and D-D' were constructed, two models for each profile. Each model combined gravity and magnetic data anomalies to help constrain the model.

GEOLOGY AND TECTONICS

The Mid-continent Rift System (MCRS) is a failed rift system that developed about 1.1 billion years ago, apparently in response to stresses associated with the Grenville Orogeny (Donaldson and Irving, 1972; Woelk and Hinze, 1991; Whitmeyer and Karlstrom, 2007). The MCRS is composed of three large-scale components; the western arm through Minnesota, Iowa, and Kansas; the Lake Superior arm; and the eastern arm through Michigan (Wold and Hinze, 1982; Van Schmus and Hinze, 1985; Shen et al., 2013) (Fig. 1). The southern limit of the eastern arm is usually placed in southeast Michigan, but a series of N-S trending gravity maxima may be a continuation of this arm into Ohio, Kentucky, and Tennessee (Van Schmus and Hinze, 1985). Lidiak and Zietz (1976) also suggested the presence of related rifts in the eastern Kentucky area. This study focuses on the western arm, especially the Iowa portion of the MCRS (Fig. 1).

The 2000 km long MCRS is comparable in length to the presently active East African and Baikal rifts (Merino et al., 2013). Although the Iowa portion of the MCRS is considered to be one of the most significant segments of the whole rift, it has been less studied than the Lake Superior segment due to the large thickness of the Phanerozoic sediments covering it (Hinze et al., 1997). Consequently, its location and geological features have been interpreted mostly by means of geophysical studies especially gravity, magnetic anomalies and seismic reflection profiles, extrapolation from the outcrops area, and a few basement drill holes (Bickford et. al., 1986; Merino et al., 2013).

2.1 Regional Tectonic

There are several questions still concerning the evolution of the MCRS. Much of the development of the MCRS apparently took place over a geologically short period of time (Van Schmus and Hinze, 1985; White, 1997; Anderson, 1992; Stein et al., 2015). Windley (1989) proposed that the MCRS may have been produced by an episode of the late Middle Proterozoic Grenville orogenic activity in much the same way that the Rhine Graben was produced by the Cenozoic Eocene Alpine Orogeny. Another hypothesis of the MCRS formation is the rift was part of an evolving plate boundary system rather than an isolated episode of midplate (Merino et al. 2013).

The MCRS region can be separated into distinct crustal terranes (provinces) (Fig. 2). The oldest terrane, the Archean Superior province of the Canadian Shield, can be subdivided into a northern granite-greenstone terrane (2.6-2.8 Ga (billion years)) and a southern gneiss-migmatite terrane (2.6-3.6 Ga) which had been highly deformed during earlier orogenies (Morey and Sims 1976; Woelk, 1989). The 1830-1890 Ma (million years) Penokean province is comprised of gneissic and metasedimentary rocks which truncates the Archean Superior province. The continental interior south of the Penokean province can be divided into the Eastern Granite-Rhyolite province (1440-1480 Ma), the western Granite-Rhyolite province (1340-1400 Ma), and the central plains province (1600-1800 Ma) which represent several orogenic events (Van Schmus et al., 1987).

Fig. 3 shows more detail about the different terranes that the MCRS cuts through, including the Archean Abitibi-Wawa greenstone-granite belt in the Lake Superior area, the Archean Minnesota River Valley gneiss- migmatite terrane (Minnesota Terrane) of east-central Minnesota, the Early Proterozoic Penokean Volcanic Belt of Iowa and

Central Plains Volcanic Belt in Nebraska, and the Middle Proterozoic Mazatzal Orogenic Belt in Kansas (Anderson, 1992).

The MCRS appears to be the product of two contrasting episodes of tectonism (Keller et al., 1983; Van Schmus and Hinze, 1985), an initial tensile phase (Baker and Morgan, 1981) which is shown by the large volume of basaltic magma associated with the MCRS, and a contractional phase (Trapponnier and Molnar, 1976; Trapponnier et al. 1982; Van Schmus and Hinze, 1985) evidenced by the proximity of the Grenville Province.

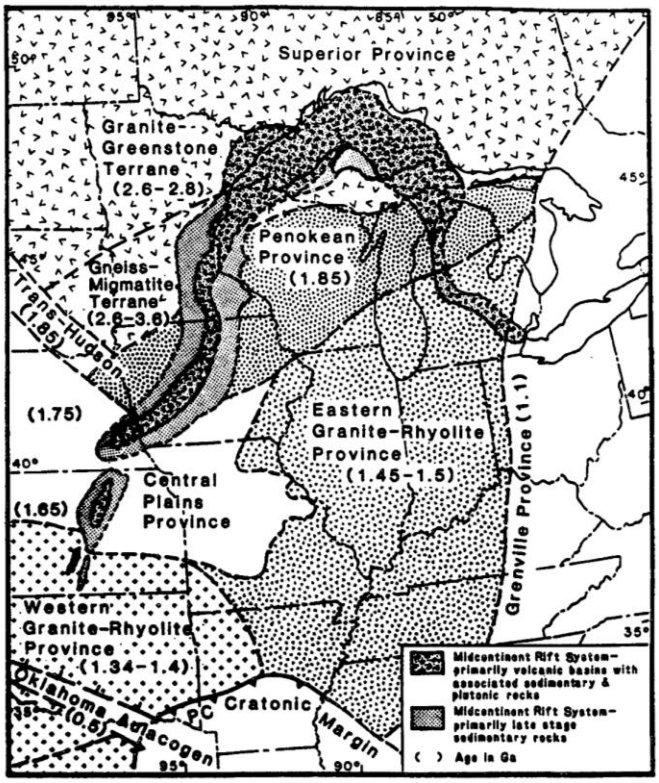

Figure 2. Basement provinces of the MCRS (Van Schmus et al., 1987; Hinze and Kelly, 1988).

Coincident with the Rodinia assembly (ca. 1.2–1.1 Ga), intracontinental extension occurred along the Midcontinent rifts (Whitmeyer and Karlstrom, 2007) including the

MCRS (Fig. 4), as shown by regionally significant extensional faults (red lines on Fig. 4) that occur throughout southern Laurentia. Also, tensile stresses led to tectonic activity that affected the Lake Superior area (Franklin et al., 1980) and was a precursor to the Middle Proterozoic opening of the Grenville Ocean. Additional products of the tensile stresses are extensive intrusions of mafic dikes (Van Schmus and Hinze, 1985). Some

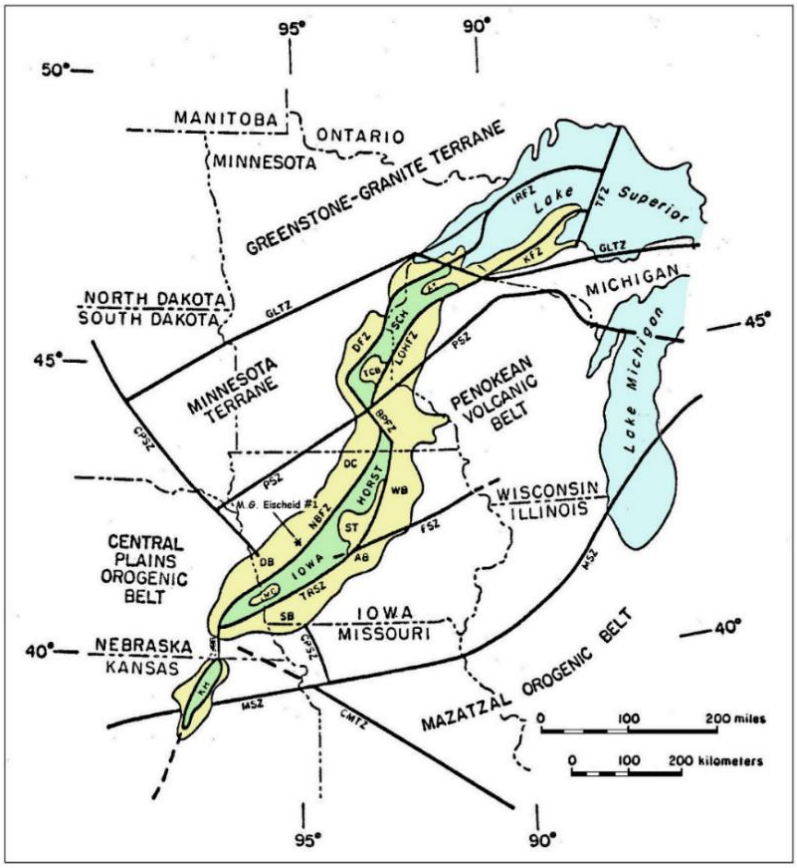

Figure 3. Structural components of the Midcontinent Rift System and related features (Anderson, 1992). TFZ=Thiel Fault Zone, IRFZ=Isle Royale Fault Zone, KFZ=Keweenaw Fault Zone, DFZ=Douglas Fault Zone, LOHFZ=Lake Owen-Hastings Fault Zone, BPFZ=Belle Plaine Fault Zone, NBFZ=Northern Boundary Fault Zone, TRSZ=Thurman-Redfield Structural Zone, BBFZ=Big Blue Fault Zone, SCH=St. Croix Horst, KH=Kansas Horst, GLTZ=Great Lakes Tectonic Zone, PSZ= Penokean Suture Zone, FSZ=Fayette Structural Zone, CPSZ=Central Plains Suture Zone, MSZ=Mazatzal Suture Zone, CMTZ=Central Missouri Tectonic Zone, ARZ= Anadarko Rift Zone, LSZ=Llano Suture Zone, AS=Ashland Basin, TCB=Twin City Basin, DB=Defiance Basin, DC= Duncan Basin, SB=Shenandoah basin, AB=Ankeny Basin, WB=Wellsburg Basin, ST=Stratford Basin, MB=Mineola Basin. (Anderson, 1992).

intrusive rocks occurred west and south of Hudson Bay (Mackenzie dikes) (Le Cheminant and Heaman, 1990) and in the Minnesota region (Animikie dikes) which are thought to be related to extensional tectonics. The positive gravity and magnetic anomalies in northeast Iowa that have been interpreted as mafic plutons are possibly associated with the MCRS (Heathcote, 1979).

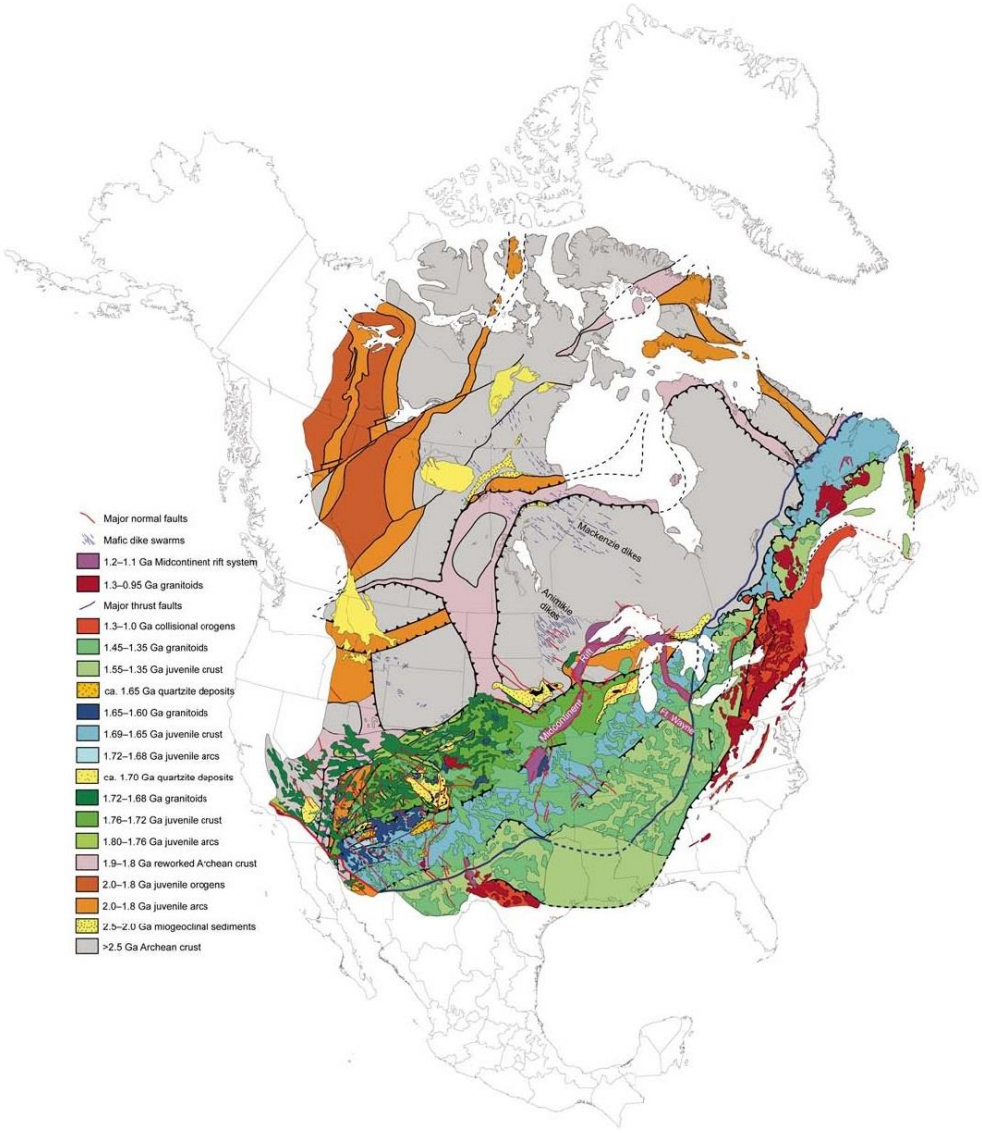

Figure 4. Intracontinental extension occurred along the Midcontinent rifts coincident with Rodinia assembly (ca. 1.2–1.1 Ga), (including the Keweenawan and Fort Wayne rifts). Regionally significant extensional faults (red lines) occur throughout southern Laurentia. Extensive intrusions of mafic dikes (dark blue lines) occurred west and south of Hudson Bay (Mackenzie dikes) and in the Minnesota region (Animikie dikes) (Whitmeyer and Karlstrom, 2007).

Donaldson and Irving (1972) and Gordon and Hempton (1986) constructed tectonic origin models of the MCRS were related to the Grenville Province to illustrate the stresses that led to the creation of the MCRS. Cambray and Fujita (1991) and Anderson (1992) describe the rift mechanism by the Slab Drag Model (Fig. 5) that involves the collision of the Grenville Craton with North America along an irregular east-dipping suture.

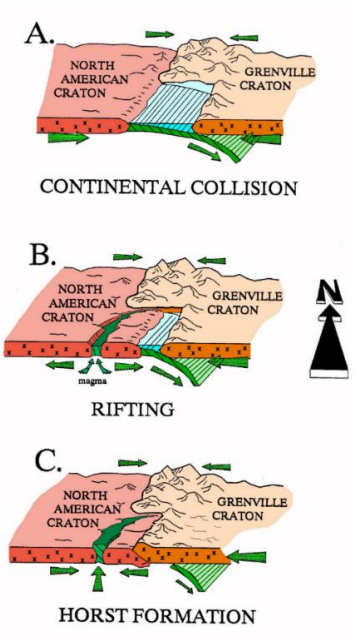

Figure 5. Illustration of the slab drag model for the formation of the MCRS (Cambray and Fujita, 1991).

Along the northern end of the MCRS, the subducting North American oceanic crust is consumed and this led to continent-continent collision; along the southern end, the subducting of the oceanic crust continued with tensile stresses that led to the MCRS formation; after consuming of the North American oceanic crust along the southern end of the suture, the eastern continental mass collided with the continental rocks of the rifted southeast corner of the north America causing the reversal of the normal displacements

along the MCRS central grabens-bounding faults and uplifting of the central horsts including the Iowa Horst.

Anderson (1992) developed another model which is the block rotation model (Fig. 6) based on the earlier ideas of rotation of the southeastern corner of the North American Craton (Donaldson and Irving, 1972). This model assumes that there is an oblique continental collision along the Grenville Suture and related strike-slip movements along an irregular zone with a constraining bend. A north-south directed maximum principal compressive stress related to the Llano Orogeny could have acted to reverse the rotation of the southeastern block, forcing up the MCRS axial horsts.

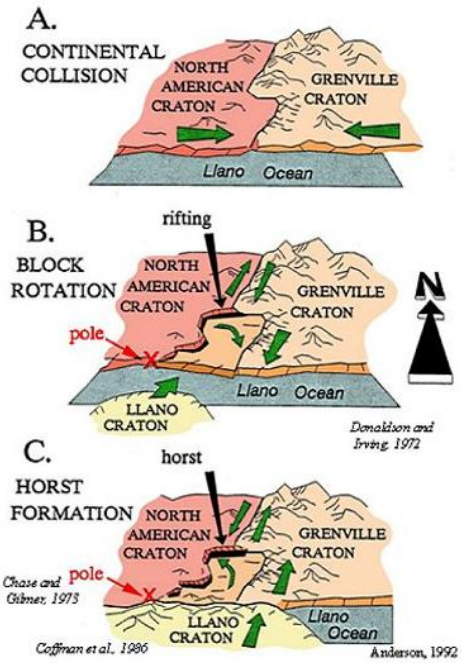

Figure 6. Illustration of the block rotation model for the formation of the MCRS (Anderson, 1992).

More recently, Stein et al. (2015) costructed a detailed model of the tectonic evolution of the MCRS (Fig. 7) and incorporated the two stages of tectonic evolution stated by Keller et al. (1983),; an initial tensile stage that was followed by a

compressional stage which is suggested by the reversal of the normal displacements (Fig. 5). Although there are models and hypotheses illustrating the tectonic evolution, a debate still exist around the tectonic evolution of the MCRS (Merino et al., 2013). The uncertainties concern the magma source; was it a mantle plume from a continental interior as the petrologic and geochemical models favor (Vervoort et al., 2007) or was it a part of the Grenville Orogeny (Fig. 5) and (Fig. 6) as included in several tectonic models (Donaldson and Irving 1972; Gordon and Hempton, 1986; Cambray and Fujita 1991; Anderson 1992) associated with the assembly of Rodinia (Whitmeyer and Karlstrom, 2007).

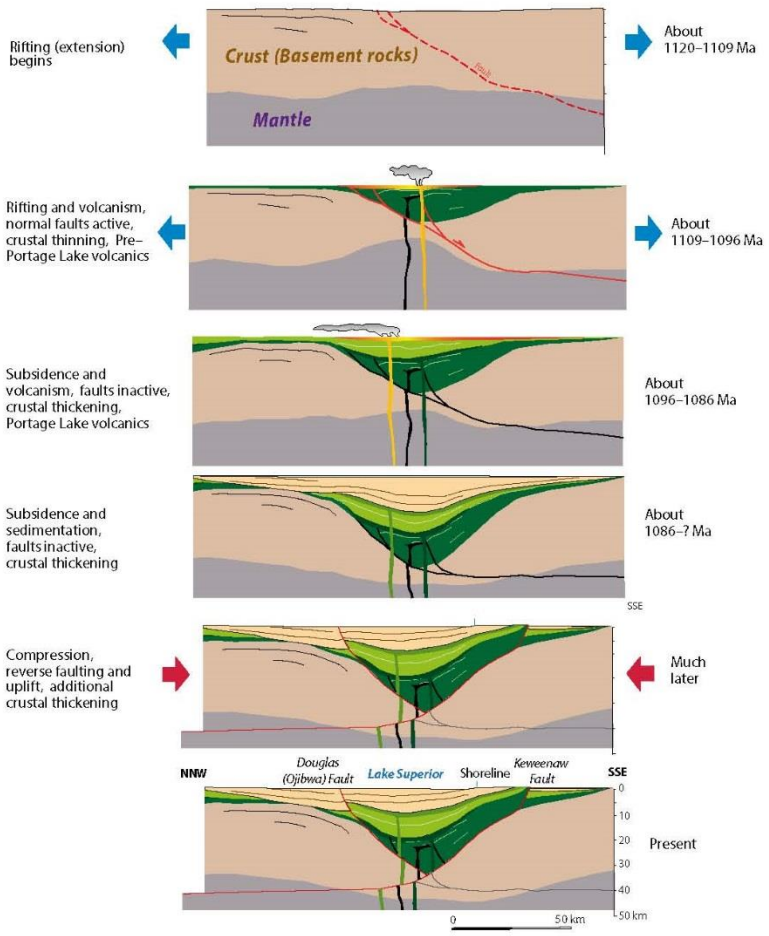

Figure 7. Schematic evolution of the Midcontinent Rift based on a model by Stein et al. (2015).

Merino et al. (2013) presented a model that the MCRS was created by magma from a microplate interaction with one end being a spreading ridge toward the west and the other end being a transform fault toward the east. However it is possible that the origin of the magma was from mantle plumes within the plate? That question is answered after a detailed study of the magma volumes along the three arms. The volume of magma increases towards the Lake Superior region and the western arm experienced significantly more magmatism (Fig. 8) indicating that it acted essentially as a spreading ridge, whereas the much smaller magma volumes along the east arm are consistent with its acting as a leaky transform (Merino et al., 2013). This view of the rift system's evolution is compatible with the rift being part of an evolving plate boundary system rather than an isolated episode of midplate volcanism being part of the Grenville Orogeny (Merino et al., 2013).

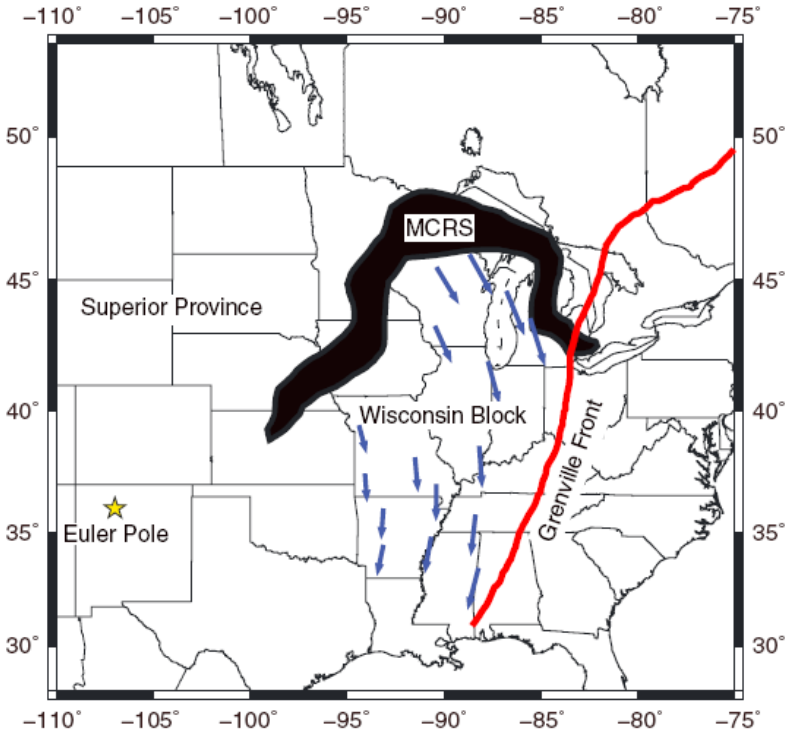

Figure 8. Schematic microplate model with the magma variations (Merino et al., 2013).

Vervoort and Green (1997) constructed a model that shows different stages of interaction of the magma with the crust (Fig. 9). In northeast Minnesota, Vervoort and Green (1997) performed an Nd isotope analysis for the North Shore Volcanic Group (NSVG) of the MCRS in order to investigate the origin of this magma. The NSVG has more felsic rocks than the other exposed volcanic rocks within the MCRS. Their analysis determined that the high felsic content of the NSVG is not due to crystal fractionation but crustal melting, specifically an evolved crustal component that must be at least late Archean in age (Vervoort and Green, 1997).

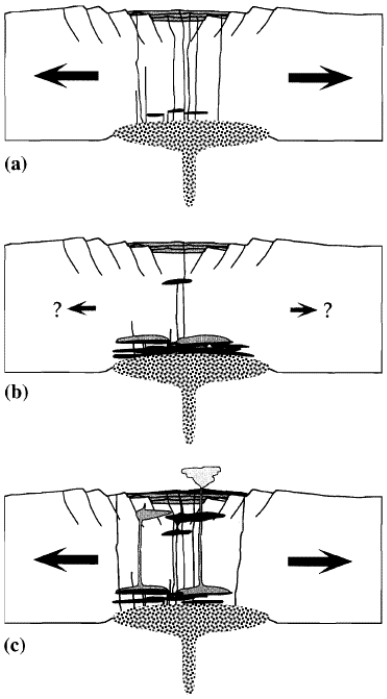

Figure 9. Model for bimodal magmatism in the MCRS. (a) Rapid extension allowing mantle-derived magmas to migrate through crust with minimal interaction. (b) Slowed or halted extension with continued supply of magma from mantle. Magma ponds at or near the base of the crust and causes widespread heating of crust and localized partial melting. Only small amounts of magma migrate to the surface during this stage. (c) Increased extension leading to renewed migration of magma through crust. Most voluminous rhyolite melts are produced or released during this stage. (Hildreth, 1981; Vervoort and Green, 1997).

2.2 Stratigraphy and Structure of the MCRS in Iowa

The MCRS rocks belong to the Keweenawan Supergroup which is composed of igneous and clastic sedimentary rocks. The MCRS lithologic units are exposed in the Lake Superior region (Van Schmus and Hinze, 1985). The Keweenawan Supergroup can be divided roughly into two groups: a primary basin fill of igneous-sedimentary unit as exposed in Duluth Gabbro and Keweenawan Volcanics with associated red clastic rocks; and a late stage fill basins overlaying the initial rock unit (Van Schmus and Hinze, 1985; Woelk, 1989).

The structural geometry of the MCRS is characterized by an aligned series of axial horsts dominated by mafic extrusive rocks (Figs. 3, 11) which are composed of basalts, basaltic andesites, olivine tholeiite, rhyolites (Fox, 1988; Woelk, T., 1989), and they are locally overlain by late rift clastics (Anderson, 1992). The volcanic rocks of the central horsts reach estimated maximum thicknesses in excess of 10.5 km (Green, 1982; Woelk and Hinze 1991; Stein et al. 2015). The horsts in Iowa are flanked by a series of asymmetric basins as shown in Fig. 10 that deepen towards the rift axis in half-graben Configurations. Those basins are bounded by normal faults and are filled with mafic volcanic and clastic sedimentary rocks, whereas the graben is affected by late stage reverse faults (Craddock et al., 1963; Behrendt et.al., 1988; Anderson, 1992).

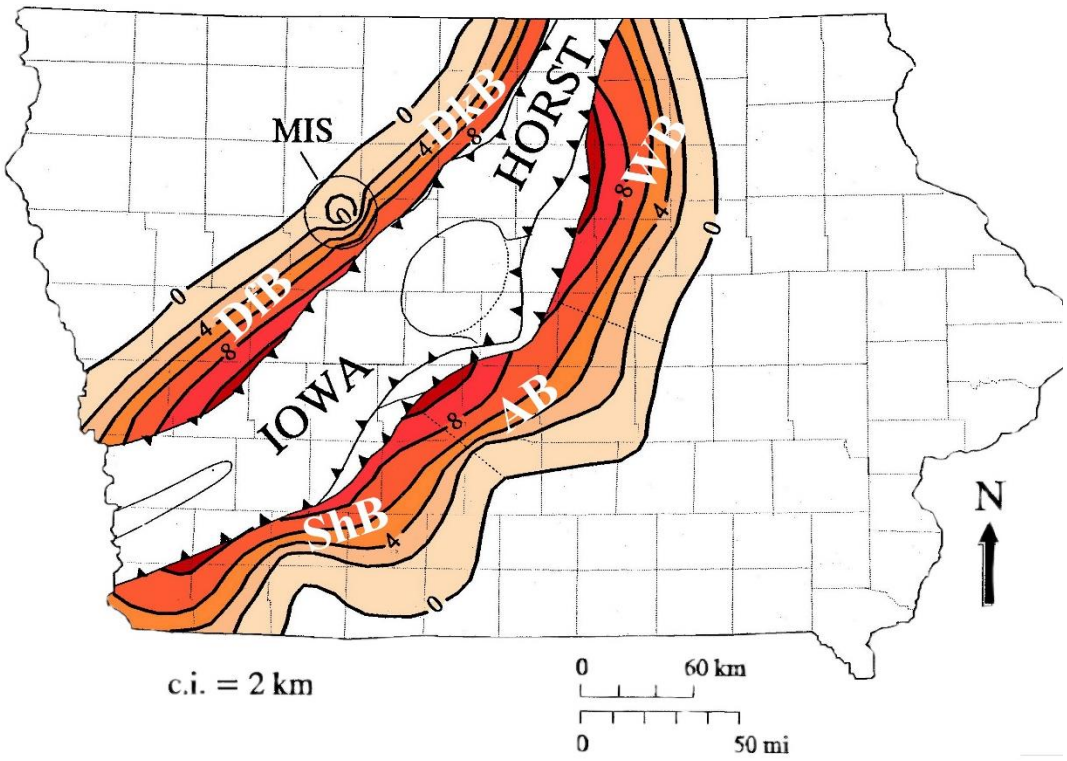

Figure 10. Total thickness map of the MCRS-related basins (Anderson, 1992). White abbreviations are the basins' names; ShB (Shenandoah Basin), AB (Ankeny Basin), WB (Wellsburg Basin), DfB (Defiance Basin), DkB (Duncan Basin).

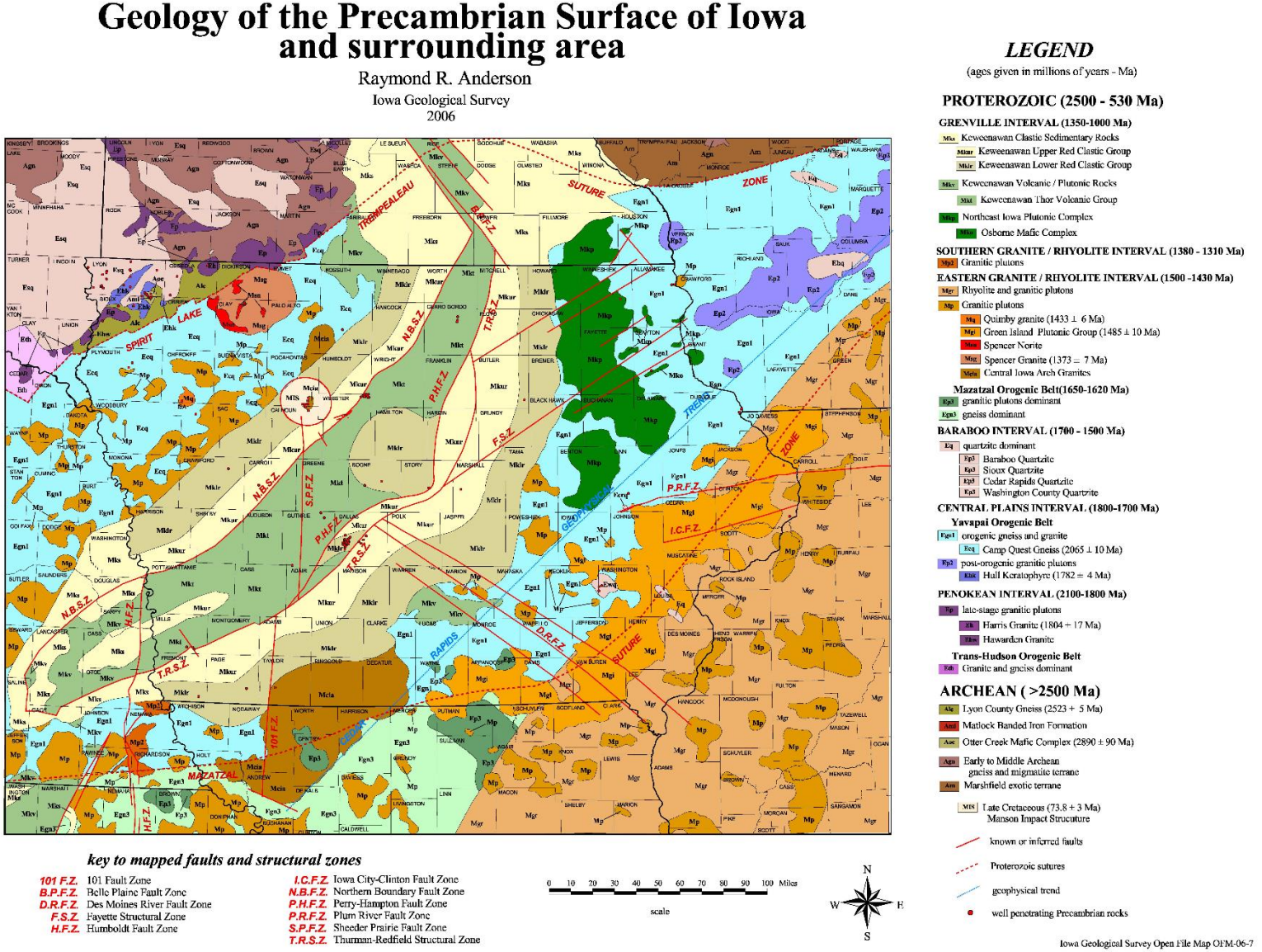

Figure 11. Geology of the Precambrian surface of Iowa and surroundings area (Anderson, 2006).

PREVIOUS GEOPHYSICAL INVESTIGATIONS

The MCRS is one of the most important tectonic features in North America. Consequently, the MCRS has been analyzed geophysically using gravity, magnetic, and seismic data since the middle 1940's. In Kansas, Woollard (1943) published the first geophysical study, a transcontinental gravity and magnetic profile that crossed the rift. Lyons (1950) published the first map that showed a large amplitude gravity anomaly extending from Kansas to Lake Superior. Ocola and Meyer (1973) identified the mafic volcanics-dominated central horst, flanking clastic-filled basins and the MCRS as a rift, based on a series of seismic refraction surveys in Minnesota, adjacent Wisconsin and Iowa based on surveys by Cohen (1966) and Mooney et al. (1970).

3.1 Broadband Seismic Studies

3.1.1 Central and Eastern United States. In the central and eastern United States, Gallegos et al. (2014) analyzed broadband seismic data from the EarthScope Transportable (TA) project. This project collected broadband seismic data from a grid of stations with a 70 km spacing, and used 39 earthquake events occurring from 2010 to 2012. Fig. 12 shows the seismic attenuation map constructed using Rayleig waves (Lg) (Gallegos et al., 2014) with the MCRS associated with a region of lower attenuation (faster seismic velocities) than the surrounding Precambrian terranes. Gallegos et al. (2014) stated that there was a positive correlation between the attenuation results and the heat flow, sediment thickness, recent tectonic activity, and crustal fluids. Additionally, the region of high attenuation south of the MCRS in Iowa might be representative of a tectonic boundary between the Yavapai and Mazatal orogenies. Along the western

segment of the MCRS in Iowa, Moidaki et al. (2013) used receiver function analysis to obtain the crustal thicknesses (Fig. 13).

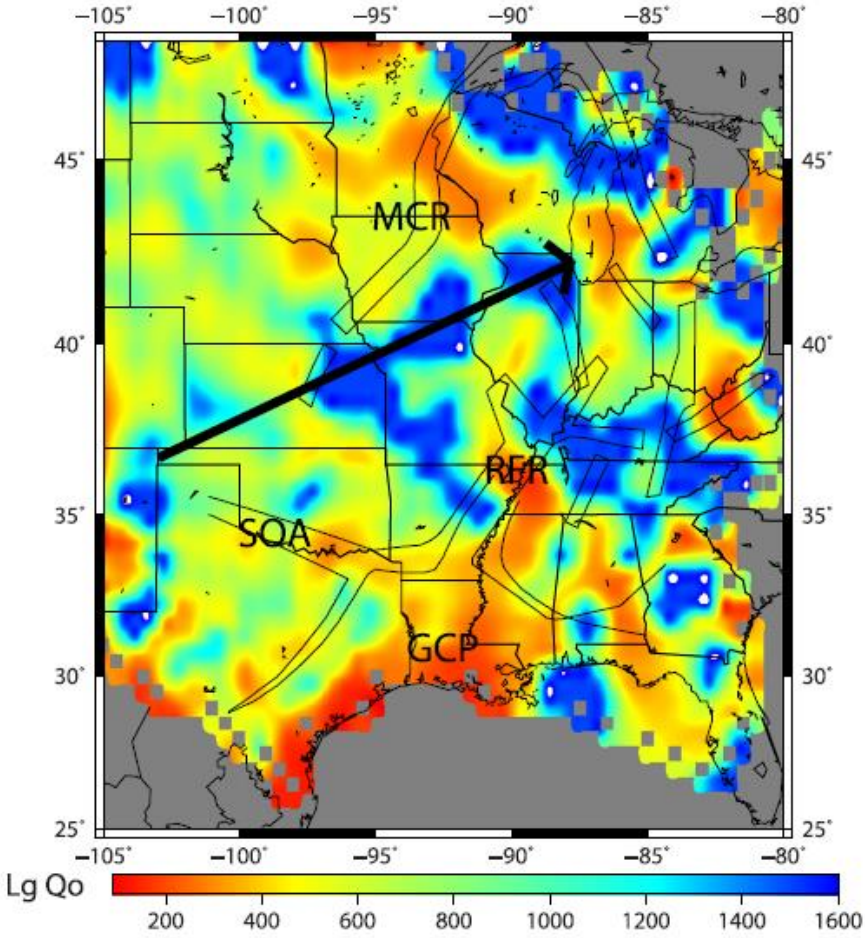

Figure 12**.** Two station Lg attenuation map (Gallegos et al., 2014). Blue represents areas of low attenuation and red represents areas of high attenuation. Thin black lines indicate rift features. Important features are labeled: MCR- Midcontinent Rift, SOA- Southern Oklahoma Aulacogen, RFR- Reelfoot Rift, and GCP- Gulf Coastal Plain. The large black arrow represents the northeast trend of low attenuation.

3.1.2. Western Arm of the MCRS. Shen et al. (2013) studied the western arm of the MCRS using Rayleigh wave data from the Earthscope project to produce a 3-D Vsv model for the crust and uppermost mantle (Fig. 14a). More than 120 TA stations were used to generate high-resolution Rayleigh wave phase velocity maps of periods between

8 and 80s. The data were jointly inverted using phase velocity dispersion curves and seismic receiver functions to determine lithospheric velocity variations (Fig. 14b). Fig. 14b shows profile B-B' (Fig. 14a) in southwestern Iowa where high velocity material occurs nearer to the surface under the MCRS than compared to other regions.

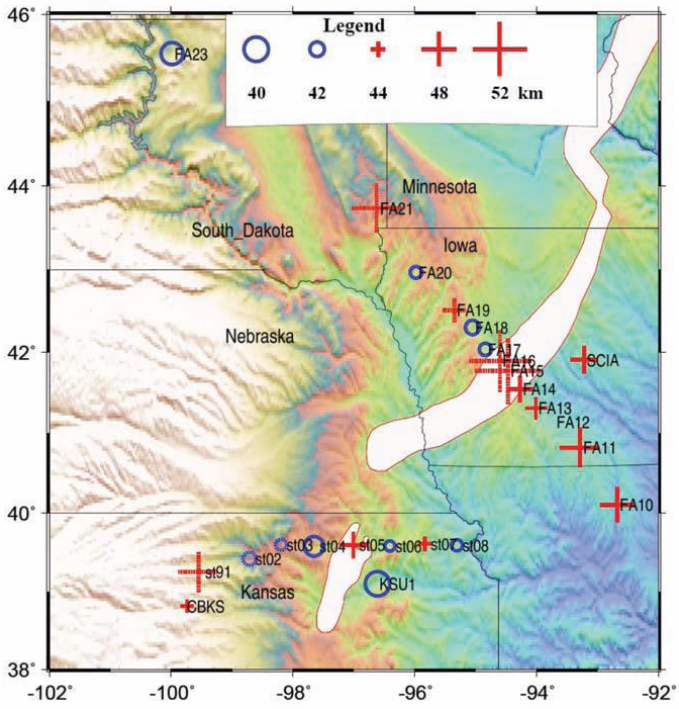

Figure 13. The crustal thicknesses across the Iowa segment of the MCRS obtained from receiver function analysis (adopted from Moidaki et al. 2013).

Although there is a lack of the vertical resolution below 150 km, the crustal thickness is determined within ranges from about 35 to 48 km and the model is divided into three principal layers: 1) a top layer being the sedimentary layer, 2) a second layer consisting of the crystalline upper and lower crust, and 3) a third layer being the uppermost mantle (Shen et al., 2013). The crust is thicker under the MCRS and higher velocities are seen in the upper mantle. Additionally, from the surface wave analysis, high surface velocities (orange) correlate to the near surface basalts of the MCRS.

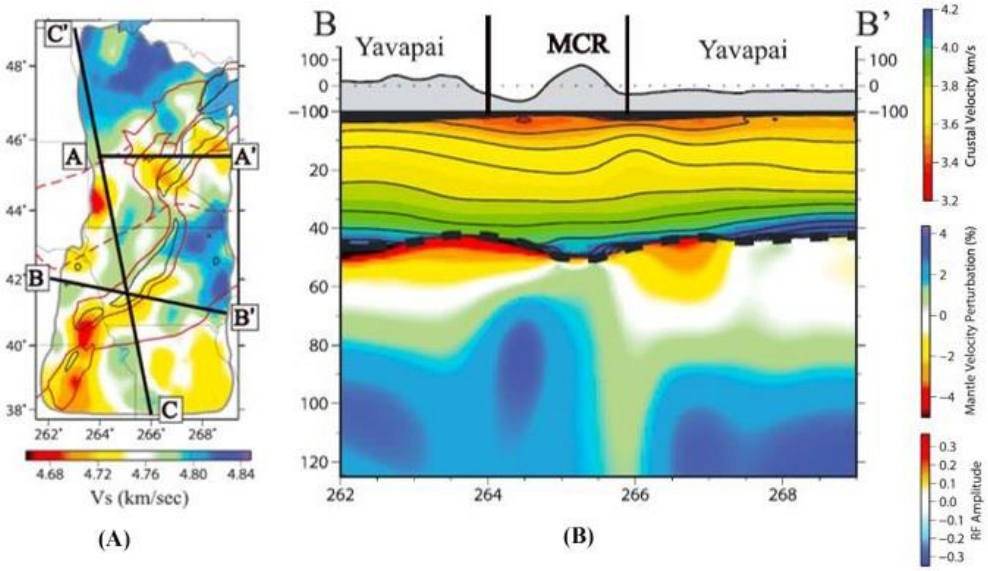

Figure 14. a) 3D seismic velocity model slice at 120 km with the locations of three profiles that cross the MCRS, b) Seismic velocity model for profile B-B'. The Moho is identified by the thick dashed line (adapted from Shen et al., 2013).

3.2 Integrated Gravity, Magnetic and Seismic Study in Northeastern Kansas

Woelk and Hinze (1991) integrated gravity and magnetic data, the deep seismic reflection data from the Consortium for Continental Reflection Profiling (COCORP) project (Serpa et al., 1984) and available drillhole results to define a crustal model of northeastern Kansas across the MCRS (Fig. 15). This integration indicated an asymmetrical basin bounded by reverse faults and with thickened crust beneath the rift. MCRS seismic reflection profiles have been interpreted by Serpa et al. (1984), Zhu and Brown (1986), Behrendt et al. (1988), Nyquist and Wang (1988), Fox (1988), Chandler et al. (1989), and Hinze et al. (1990) at various locations from Kansas to Lake Superior. They found that along the original normal faults, the graben structure is complicated by late-stage reverse movement of as much as 5 km. During the rifting event, the upper crust was thinned but was thickened by a large volume of volcanic and sedimentary rocks in the rift basin. In the eastern Lake Superior region, the total rift-rock package reaches a

maximum thickness of 30 km, where 20 km of volcanic rocks are overlain by 10 km of clastic sedimentary rocks; a total thickness in excess of 10 km is common along the rift.

Based on Fig. 15, the rift basin reaches a maximum depth of 9 km on northeastern Kansas, the throw on the reverse faults on either side of the rift basin is 3 km, and based on small scale, high amplitude reflections in the upper and lower crust, the MCRS mafic material is not a continuous body but lens of intruded material scattered throughout the crust (Woelk and Hinze, 1991). This model shows underlying mafic material within the upper and lower crust is not continuous but may consist of isolated regions of mafic materials.

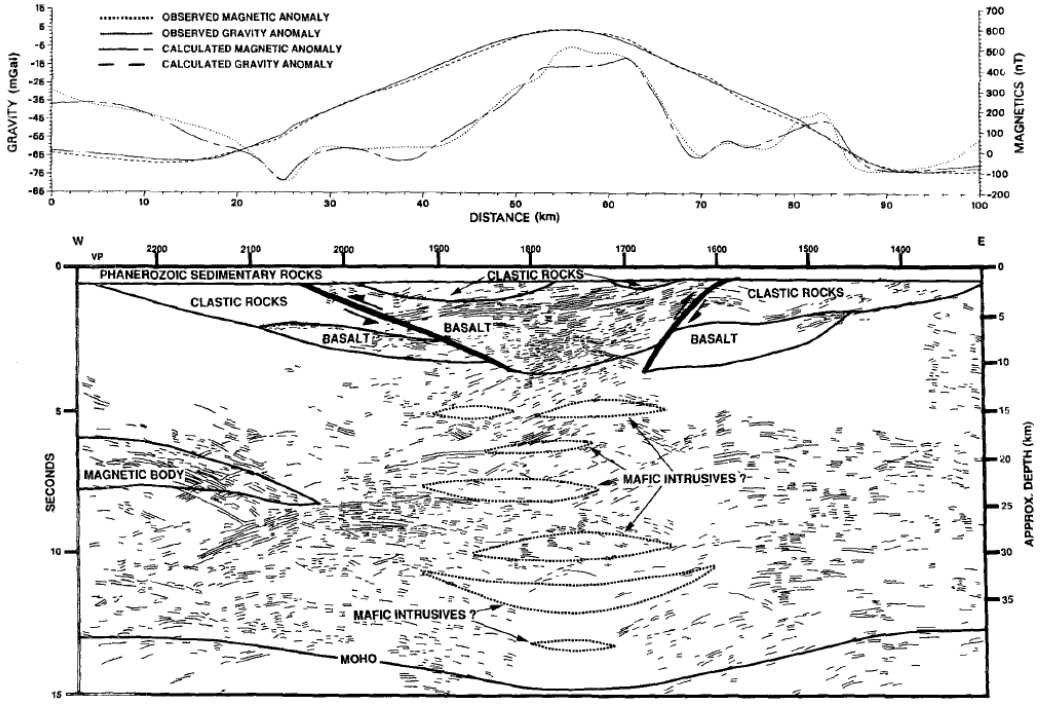

Figure 15. Geologic model based on a combined gravity and magnetic model of the interpreted COCORP seismic reflection Kansas line 1 with the calculated and observed gravity and total field magnetic anomalies (Woelk and Hinze, 1991).

3.3 Gravity, Magnetic and Seismic Studies in Lake Superior and Iowa

3.3.1 MCR Deep Crustal Structure in Lake Superior Region. The GLIMPCE (Great Lakes International Multidisciplinary Program on Crustal Evolution) project recorded six 24- to 30-fold seismic reflection profiles across the MCRS in Lakes Superior and Michigan in 1986 to study the distribution and geometry of the deeper reflections and their relation to the rift basin (Behrendt et al., 1988) (Fig. 16).

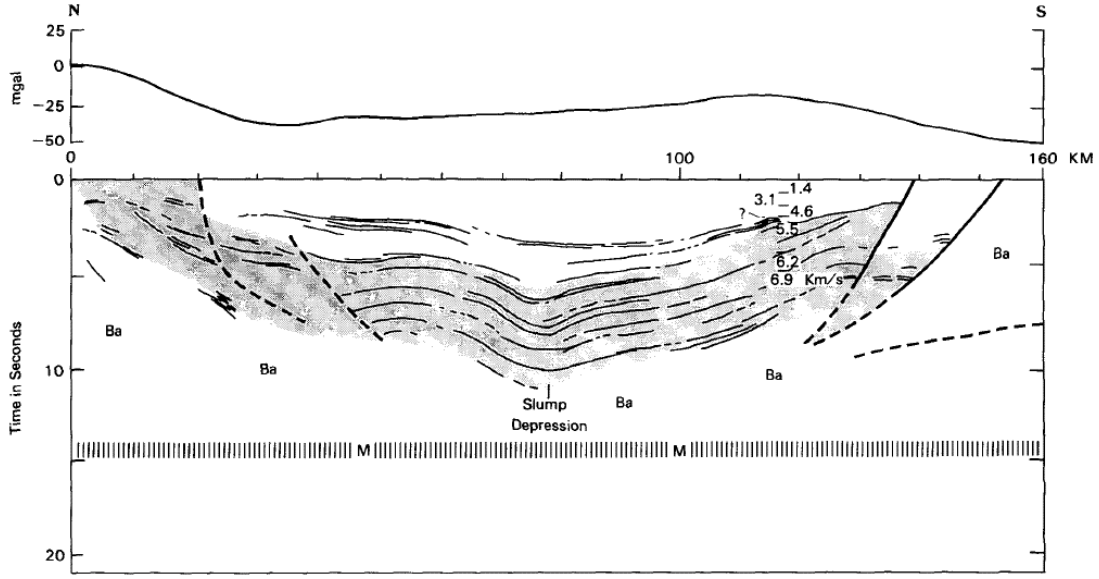

Figure 16. Interpreted seismic reflection profile with a Bouguer gravity profile in Lake Superior (Wold and Hinze, 1982). Vertical hachures outline transition from crust to mantle, steep dashed and solid lines indicate interpreted faults (Behrendt et al., 1988). Numbers represent seismic P-wave velocities of the sediments and basalts.

The seismic reflection profiles imaged a 100-km-wide rift basin that is represented by a synclinal package of reflections and is bounded on its southern margin by two or more normal (growth) faults. Nearly flat-lying, poorly reflecting, postvolcanic clastic sedimentary rocks are predominant in the upper 12-14 km of the central rift basin (Behrendt et al., 1988).

3.3.2 Magnetic Models of the MCRS in Eastern Lake Superior. Mariano and Hinze (1993) constructed 2D forward magnetic model in eastern Lake Superior (Fig. 17). Depending on intensive paleomagnetic studies, the basalts possess a normal remnant magnetization within the top 20% of the rift with inclination (I) = 40°, Declination (D) = 290° and it possess a reversed remanent magnetization component with inclination (I) = 60, Declination (D) = 110° (Halls 1982). The magnitude of the induced magnetization they used = 2.9 A/m, the magnitude of the remanent magnetization = 4.5 A/m.

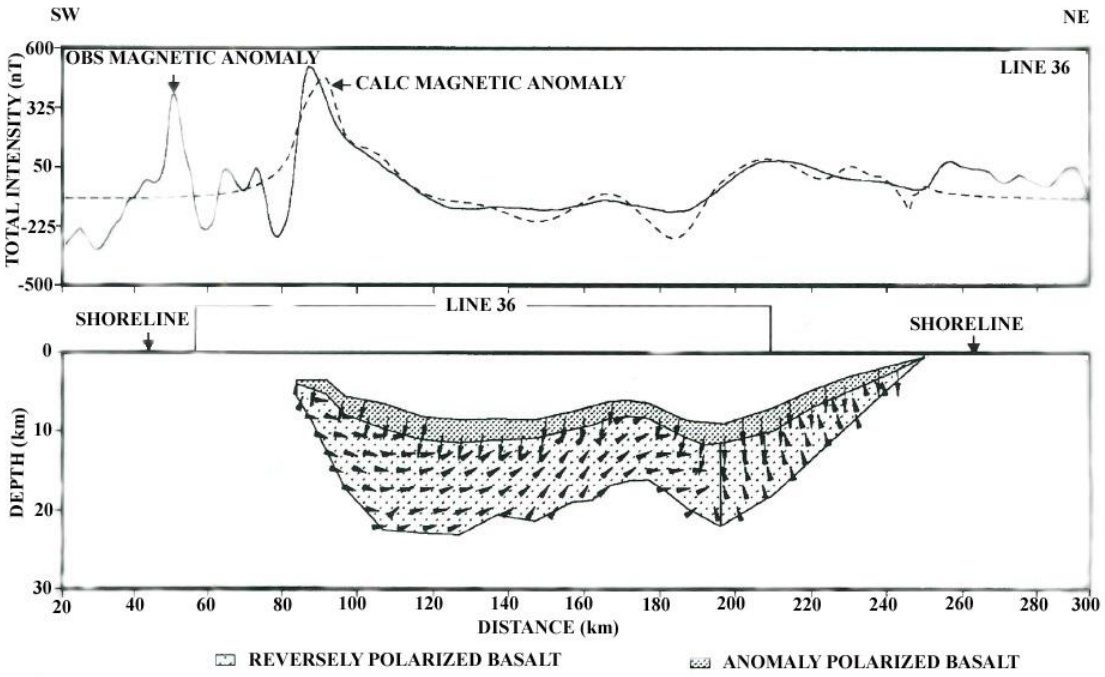

Figure 17. 2D forward magnetic model eastern Lake Superior. The vectors indicate the direction of the profile. Magnitude of induced magnetization = 2.9 A/m; magnitude of remanent magnetization = 4.5 A/m. (Mariano and Hinze (1993).

3.3.3 Gravity and seismic analysis in Iowa. Anderson (1992) performed a detailed geophysical study of the MCRS in Iowa using gravity and seismic reflection data. He constructed eleven gravity models across the MCRS (Fig. 18) with seven profiles (profiles 7, 8, 9, 10, 11, 12, 13) along seismic reflection profiles that help

constrain the interpretation of the gravity and magnetic models. The four other models (a-a', b-b', c-c', d-d') do not have any seismic reflection constrains.

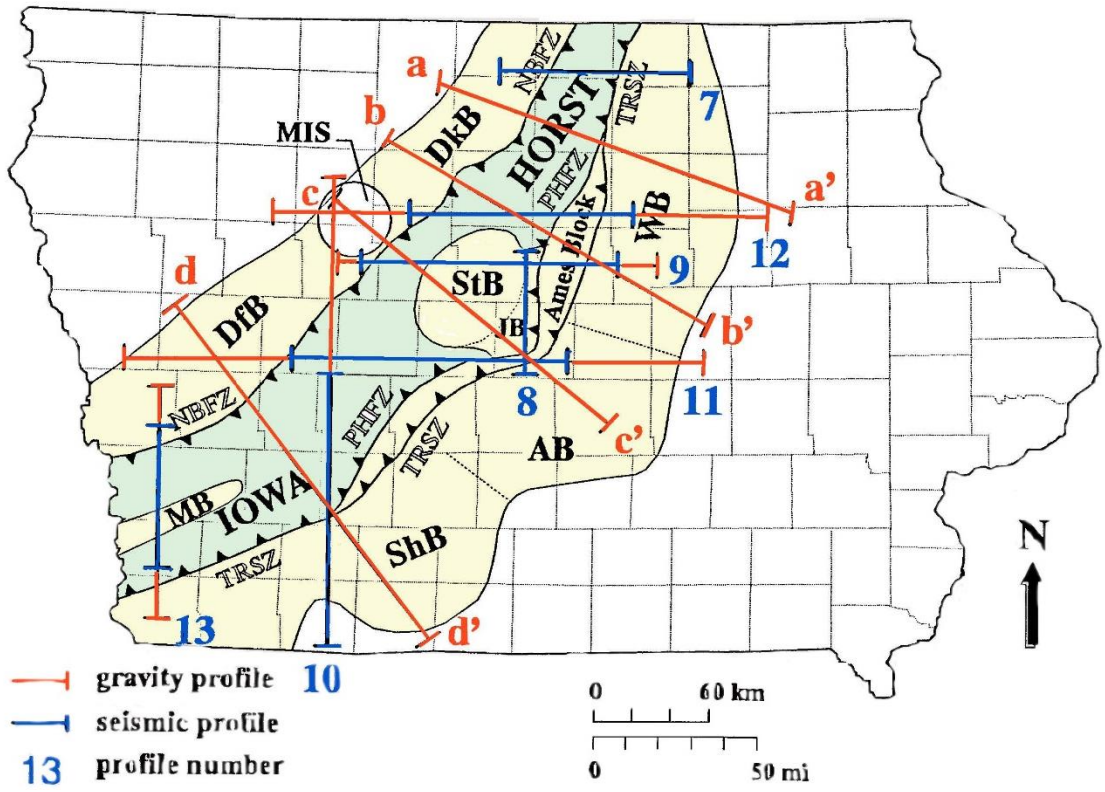

Figure 18. Location of the gravity and seismic profiles used by Anderson (1992) to construct crustal models of the MCRS in Iowa. Also shown are the different structures of the MCRS including WB=Wellsburg Basin, DKB= Duncan Basin, DfB=Defiance Basin, ST=Stratford Basin, AB=Ankeny Basin, ShB=Shenandoah basin, MB=Mineola Basin. TRSZ=Thurman-Redfield Structural Zone, NBFZ=Northern Boundary Fault Zone, BPFZ=Belle Plaine Fault Zone.

Seismic reflection profile 12 (Fig. 19a) includes 6 seconds of data with an approximation of a true depth cross section (Fig. 19b). Both Upper and Lower Red clastic sequences (PCuc and PClc) are separated by an indistinct angular unconformity. The Lower Red Clastic sequence reflectors are differentiated from those of the Upper Sequence by their more continuous, wavy parallel reflections. There are no reflectors

indicative of lava flows at the base of the clastic sequence, and the basement is interpreted as dominantly granitic metasediments and intrusive rocks.

Based on the interpretation of seismic reflection profile 12 (Fig. 19), Anderson (1992) was able to construct a gravity model (Fig. 20). Even though the seismic reflection profile did not image the crust/mantle boundary, he used as a constraint a 48 km thickness determined by Allenby and Schnetzler (1983). Additionally, Anderson (1992) broke the crust into three main layers: 1) upper crust (surface – 12.8 km), 2) middle crust (12.8 – 23 km), and 3) lower crust (23 – 48 km) where the densities and seismic velocities he used are shown in Table 1.

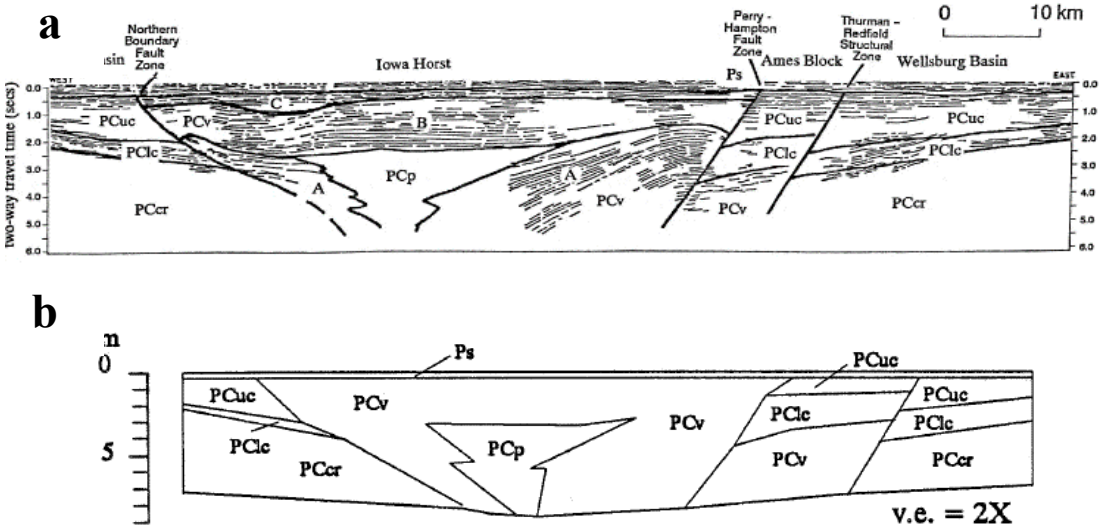

Figure 19. Interpretation of seismic reflection profile 12 (Fig. 18) (Anderson, 1992). a) The interpreted time cross section, .and b) the interpreted depth cross section. Ps=Paleozoic sediments, PCv=Keweenawan volcanics, PCuc=Keweenawan Upper Red Clastic Sequence, PClc=Keweenawan Lower Red Clastic Sequence, PCp= Keweenawan pluton, PCcr=pre-Keweenawan crystalline rocks (adapted from Anderson, 1992).

A gravity model (Fig. 20) shows that the Wellsburg Basin clastic fill reaches a maximum depth of 7.5 km, the PCuc has a thickness of 4.8 km, the PClc reaches a maximum thickness of 3.7 km, and the lithologies on the eastern edge of the Iowa Horst

are thrust over the clastic sequence within the Wellsburg Basin along the Thurman-Redfield Structural Zone. The Ames Block has an apparent width of about 15 km. The PClc sequence on the Ames Block thickens to the west, ranging in thickness from 2.7 km to about 3.8 km. West of the Perry-Hampton Fault Zone, the Iowa Horst is dominated by mafic volcanic rocks as evidence by the disturbed reflectors interpreted on the seismic reflection profile as a region of mafic plutonic rocks, and modeled with a density of 3.08 g/cc (Anderson, 1992).

Table 1. Densities and seismic velocities used in modelling of MRS profiles in Iowa. Adopted from Anderson (1992).

Lithologic Unit	Velocity (ft/sec)	Density (gm/cc)
Phanerozoic sediments	9000	2.44
Upper Keweenawan clastics	13200	2.40-2.45
Lower Keweenawan clastics	15800	2.70-2.75
Keweenawan mafic rocks		
Upper crust volcanics	19800	2.90
Middle crust Gabbro	- -	2.97
Lower crust zone of dikes	- -	3.00
Granitic plutons		
Upper crust	- -	2.67-2.68
Middle crust	- -	2.79
Pre-rift crystalline basement		
Upper crust	- -	2.74-2.78
Middle crust	- -	2.81-2.85
Lower crust	- -	2.88

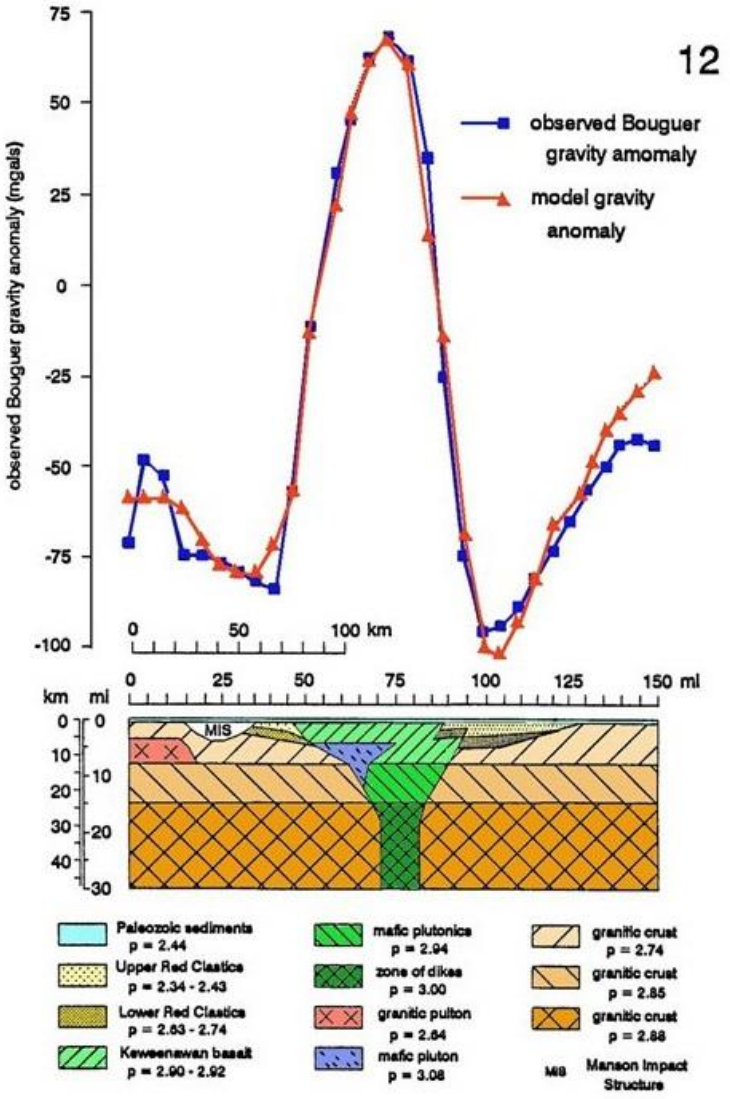

Figure 20**.** Two dimensional gravity model of gravity profile 12 (Fig. 18) with the observed and calculated Bouguer gravity anomalies (Anderson, 1992).

3.4 Gravity Analysis in Southwestern Iowa

The MCRS is characterized by a high amplitude gravity anomaly as a result of thick sequence of dense mafic-dominated volcanic and plutonic rocks and low amplitude gravity anomaly that is produced by the thick sequences of less dense, rift-related, clastic sedimentary rocks that are preserved in a five clastic-filled basins marginal to the horst

(Fig. 18) (Anderson, 1981). Anderson (1992) constructed four gravity models (Fig. 21) in southwestern Iowa that are not constrained by seismic reflection profiles. Profile d-d' crosses the Defiance Basin, the Iowa Horst, and the Shenandoah Basin as shown in Fig. 18.

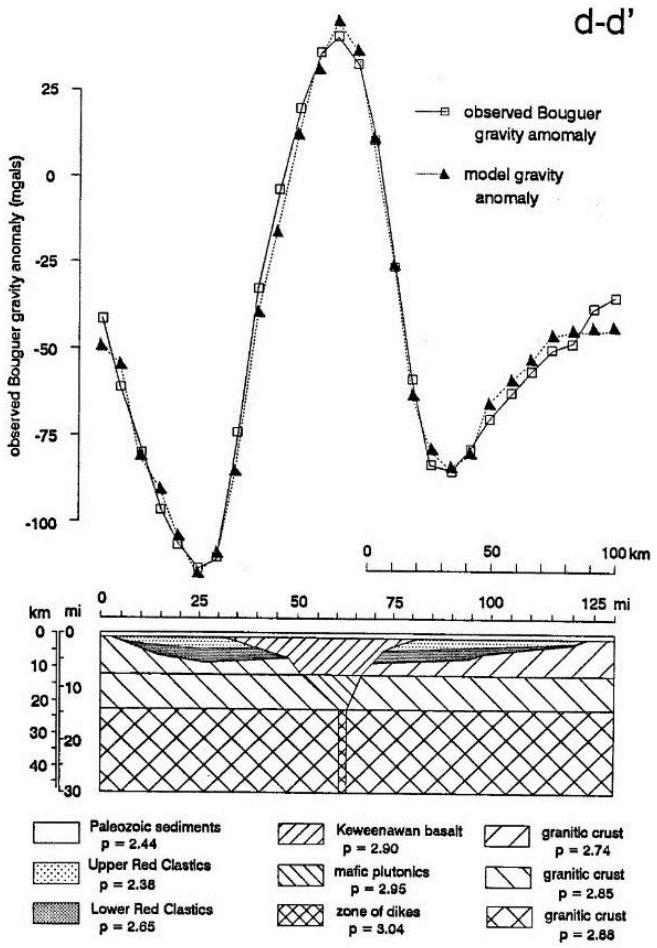

Figure 21. Two dimensional gravity model of MCRS along profile d-d' (Fig. 18) and also showing the observed and calculated Bouguer gravity anomalies (Anderson, 1992).

According to this model, the Iowa Horst shows to occur within the upper crust as an 85 km wide region that contains mafic volcanics at the Precambrian surface and narrows to 24 km at the top of the middle crust (Fig. 21). In the middle crust; the horst is comprised by gabbroic rocks narrowing to 3 km at the base of the middle crust, and in the

lower crust below the Iowa Horst as a zone of 3 km mafic dikes that continue to the base of the crust. Adjacent to the horst, the PCuc unit has a maximum thickness of 2.7 km and the PClc has a maximum thickness of 4.0 km. The Defiance Basin west of the Iowa Horst has a 4.6 km a maximum thickness of the PCuc and a 3.0 km maximum thickness of the PClc.

GRAVITY AND AEROMAGNETIC DATA

4.1. Gravity Data

The gravity data were obtained from National Geospatial and Imaging Agency (formerly Defense Mapping Agency). The location of the 13,793 gravity stations is shown in (Fig. 22). The data were reduced using the 1967 International Gravity formula (Morelli, 1976). Free-air and Bouguer gravity corrections were made using sea level as a datum and 2.67 gm/cc as a reduction density.

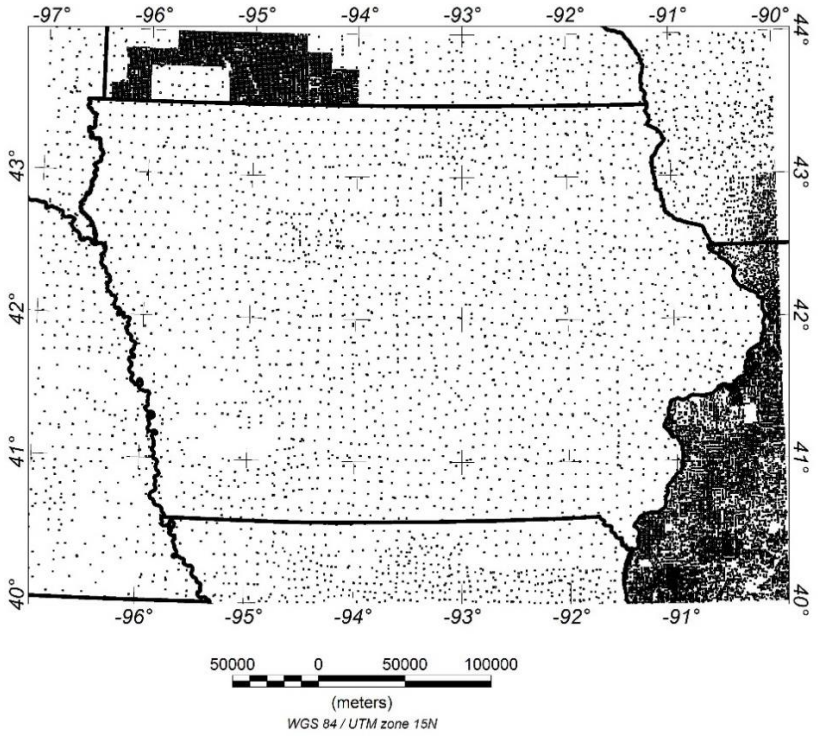

Figure 22. Location map of the gravity stations in Iowa and the surrounding areas.

The spurious points were examined and those considered to be outliers were removed from analysis. The Bouguer gravity data were gridded at a spacing of 2 km using the minimum curvature method and contoured to produce a Bouguer gravity

anomaly map (Fig. 23). This grid was used in all the subsequent map analyzes. Terrain corrections were not applied because of the lack of significant topography within Iowa.

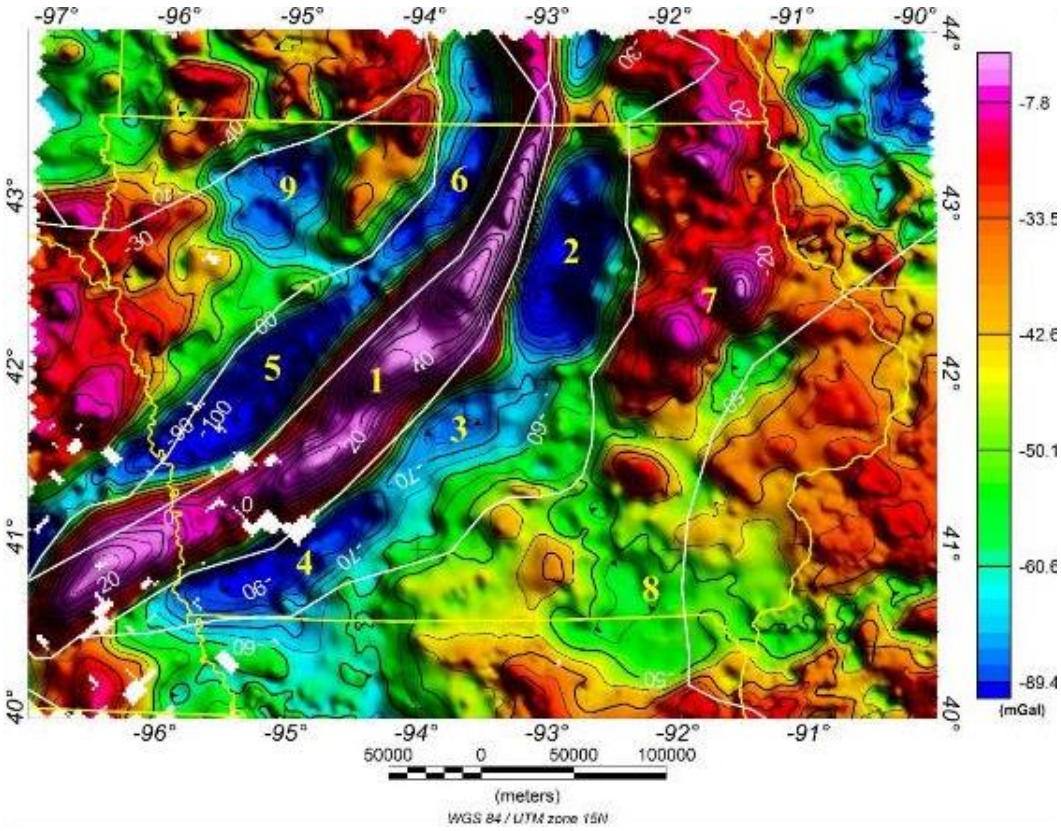

Figure 23. Bouguer gravity map of Iowa and the surrounding areas. White numbers are the Bouguer gravity values. Contour interval is 5 mGal. Yellow numbers refer to gravity anomalies mentioned in text. Yellow line are the state boundaries. The white lines are the Precambrian boundaries. White areas indicate no data acquisition.

4.2. Magnetic Data

The aeromagnetic data were obtained from the U.S. Geological Survey (USGS) (Bankey et al., 2002) who merged numerous surveys into one coherent grid with a grid spacing of 1 km. The USGS data were compiled from different surveys with varying flight elevations and International Geomagnetic Reference Fields (IGRF) removed. The data were continued either upward or downward to 1 km above the Earth's surface and an

IGRF of 2000 was then removed. The processed individual surveys were regridded into regional compilations to produce a final grid of the study area (Bankey et al., 2002). Due to the difference in survey line spacing between the original and individual surveys, the interpretation may be less accurate in some areas. The final magnetic grid was regridded at a 2 km spacing using the minimum curvature method and contoured to produce a total magnetic intensity map (Fig. 24).

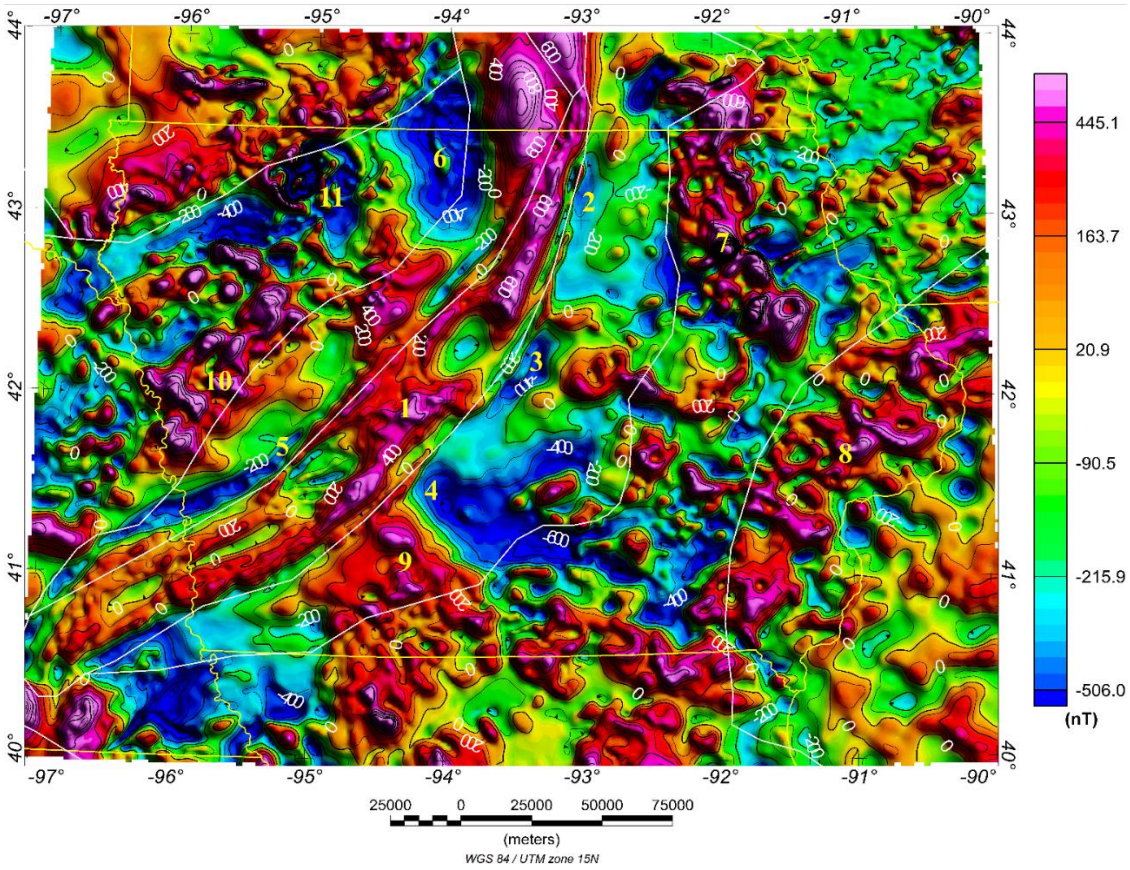

Figure 24. Total magnetic intensity map of Iowa and the surrounding areas. White numbers are the total values. Contour interval is 100 nT. Yellow numbers refer to magnetic anomalies mentioned in text. Yellow lines are the state boundaries. The white lines are the Precambrian boundaries.

GRAVITY AND MAGNETIC ANALYSIS

5.1. Gravity and magnetic anomalies

The Bouguer gravity anomalies shown on Fig. 23 can be caused by both regional and local density variations occurring at different depths (Skeels, 1967; Mickus and Montana, 1999). Consequently, to interpret the Earth's crust using gravity data, the gravity anomalies of the density variations at certain depths must be separated to obtain a residual gravity anomaly due to the distinct features that we want to study. For this purpose it is important that we compare known geologic sources with the residual gravity data.

To qualitatively interpret a region's crustal structures, we used the common enhancement method of wavelength filtering (Peeples et al., 1986). A low-pass filter emphasizes the deeper and larger scale density variations (regional gravity anomalies) and removes the shorter wavelength anomalies. A high-pass filter removes the deeper features or longer wavelength anomalies and ascertains the shallower ones (local or residual gravity anomalies), whereas a band-pass filter ascertains a certain range of wavelengths that are caused by particular geologic features at specific range of depths. Direct interpretation from the filtered maps should be avoided due to the nature of the Fourier transformation that can create false anomalies (Ulrych, 1968) due to Gibb's phenomena.

The Bouguer gravity anomaly map (Fig. 23) shows gravity anomaly values ranging from -100 to 40 mGal. A series of low-pass, high-pass and band-pass filtered maps were constructed to analyze the gravity field associated with the MCRS and the crustal structure surrounding the MCRS. A low-pass filter was constructed that passed

wavelengths greater than 120 km (Fig. 25), and a band-pass filter was constructed that passed wavelengths between 50-120 km (Fig. 26). From combinations of wavelengths ranging between 20 and 150 km, and after several trials using different wavelengths, wavelengths between 50 and120 km best represented the anomalies associated with the MCRS. The band-pass filtered gravity anomaly map was created to interpret the upper crustal gravity anomalies (Fig. 26).

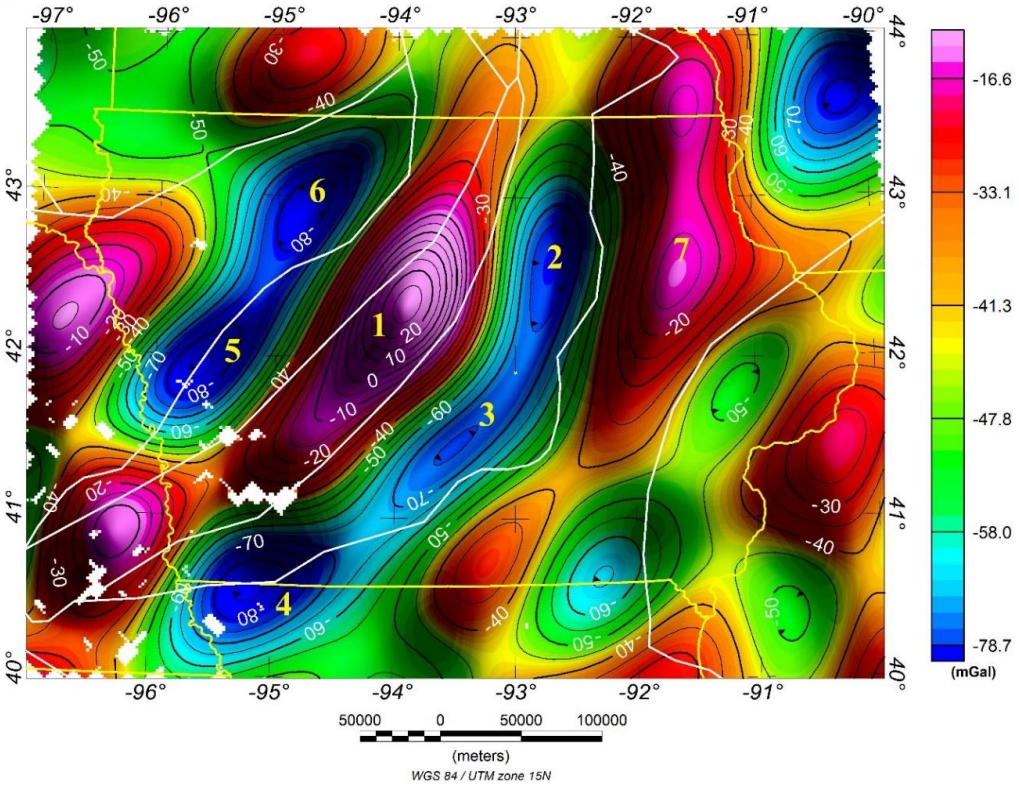

Figure 25. Low-pass filtered gravity anomaly map where wavelengths greater than 120 km were passed. White numbers refer to the low-pass filtered Bouguer gravity values. Contour interval is 5 mGal. Yellow numbers refer to gravity anomalies mentioned in text. Yellow lines are the state boundaries. White lines represent Precambrian terranes boundaries (Van Schmus et al., 1987). White areas indicate no data acquisition.

Magnetic anomaly maps mainly image the occurrence of magnetic minerals, specifically magnetite, within the Earth's crust. Consequently, magnetic maps are highly

useful in detecting the lithological variations of exposed igneous rocks and the depth to usually nonmagnetic sedimentary basins, (Phillips et al., 1993).

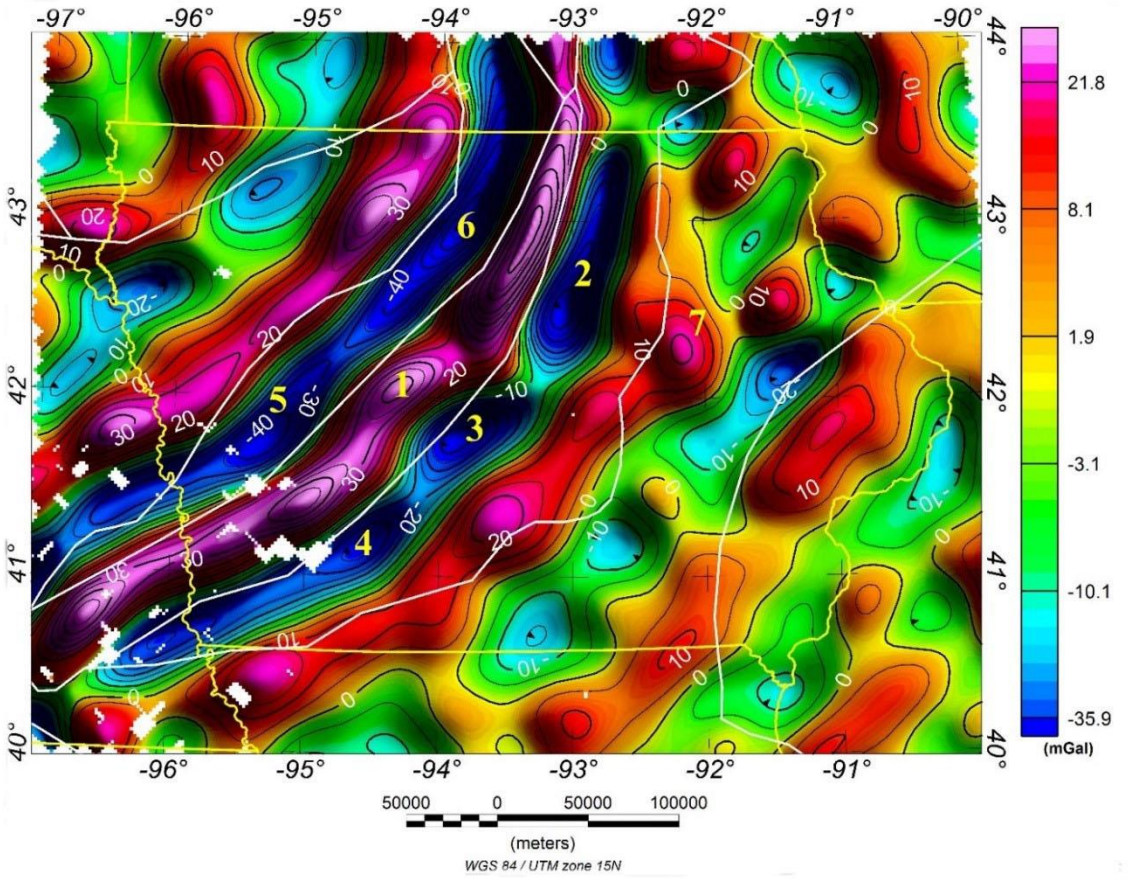

Figure 26. Band-pass filtered gravity anomaly map where wavelengths between 50 and 120 km were passed. White numbers refer to the band-pass filtered Bouguer gravity values. Anomaly 1-6 are discussed in the text. Contour interval is 5 mGal. Yellow numbers refer to gravity anomalies mentioned in text. Yellow lines are the state boundaries. White lines represent Precambrian terranes boundaries (Van Schmus et al., 1987). White areas indicate no data acquisition.

To better interpret the trend of gravity and magnetic anomalies, and to interpret the lateral boundaries of the density and magnetic susceptibility sources, one can use derivative techniques including horizontal and vertical gradients (Blakely and Simpson, 1986). A tilt derivative gravity anomaly map (Fig. 27) was constructed to detect

specifically the shape and the edge location of the causative bodies (Verduzco et al., 2004).

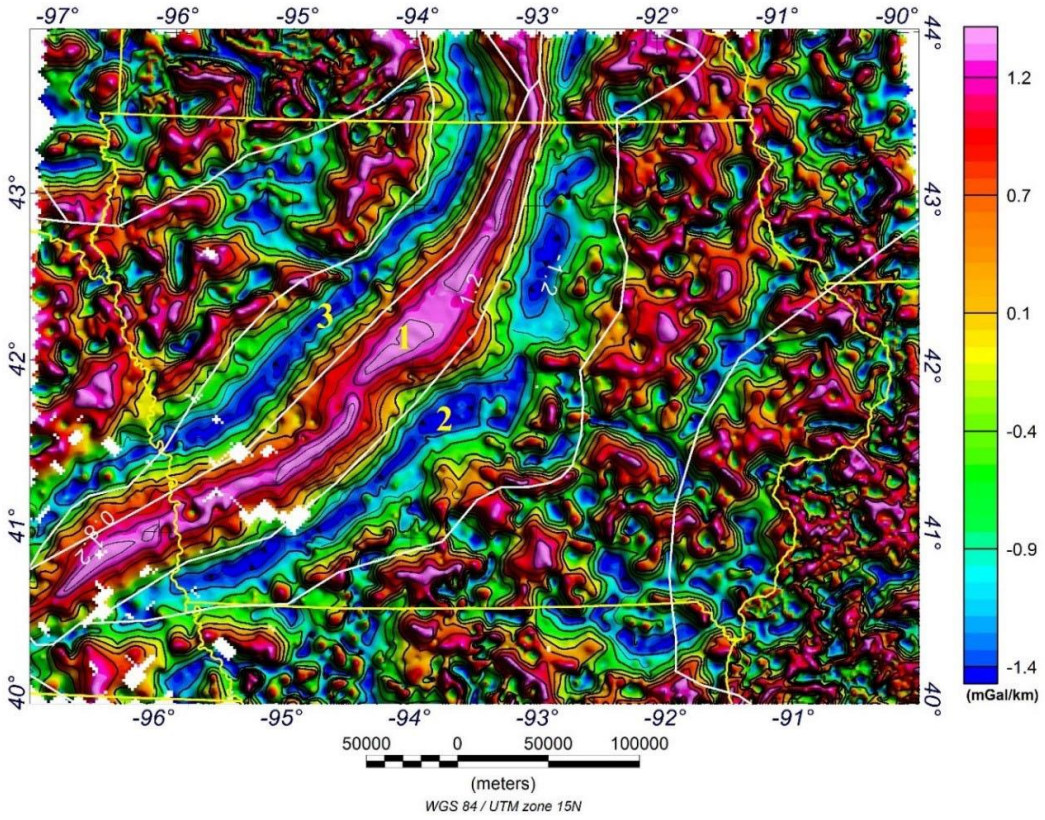

Figure 27. Tilt-derivatives of the Bouguer gravity anomaly map. White numbers refer to the gravity values. Contour interval is 0.2 mgal/km. Yellow numbers refer to gravity anomalies mentioned in text. Yellow lines are the state boundaries. White lines represent the Precambrian terranes boundaries (Van Schmus et al., 1987). White areas indicate no data acquisition.

On Fig. 27, anomaly 1 best delineates the boundaries of the main trend of the Iowa horst of the MCRS. Also, anomalies 2 and 3 (Fig. 27) around the rift sharply detect the boundary of the low gravity minima due to the rift-related basins. The detected boundaries are best fits with the white lines which represents boundaries within the Precambrian basement (Fig. 27). Using the total intensity magnetic map (Fig. 23), a

reduced to the north magnetic pole map (Fig. 28) was created to remove the effect of the dipolar nature of the magnetic field.

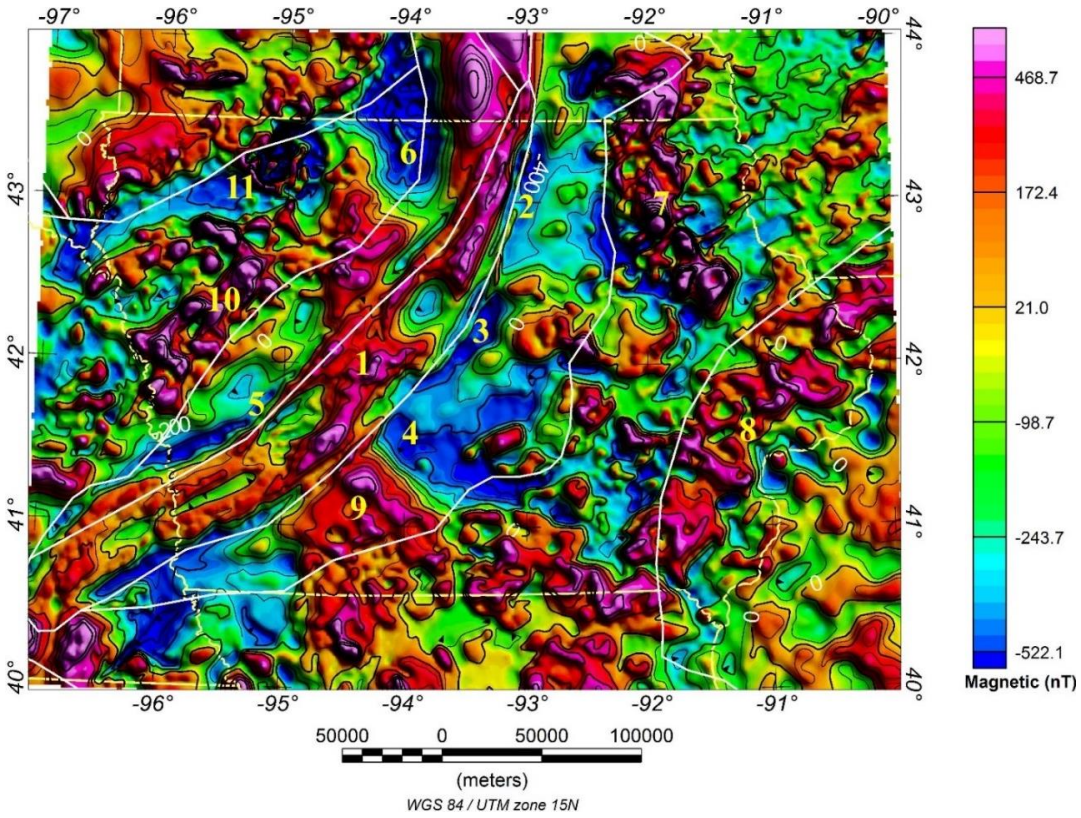

Figure 28. Reduced to the pole magnetic map of the MCRS and the surrounding area. White numbers refer to the reduced to pole magnetic values. Contour interval 100 nT. Yellow numbers refer to magnetic anomalies mentioned in text. Yellow lines are the state boundaries. White lines represent the Precambrian terranes boundaries (Van Schmus et al., 1987).

5.2. Combined Gravity and Magnetic Data Interpretation

The diverse gravity and magnetic anomalies within and around the MCRS are described in this section. Anomaly 1 (Figs. 23, 24, 25, 26, 27 and 28) is shown by a linear gravity and magnetic maximum. Gravity anomaly 1 (Fig. 23) ranges from 20 to 60 mGal in amplitude while the band-pass filtered gravity anomaly map has amplitudes ranging between 20 and 30 mGal (Fig. 26). Magnetic anomaly 1 (Fig. 24) has an amplitude of

more than 400 nT. Anomaly 1 on both the gravity and magnetic anomaly maps is produced by the Iowa horst along the entire rift as seen in the geological maps (Figs. 1, 3, 11). Based on gravity modeling, the Iowa horst is thought to be sourced by a thick (~30 km) volume of volcanic rocks (Hutchinson et al., 1990; Merino et al. 2013), with the volcanic rocks being composed of basalts and basaltic andesites (Green, 1982; Fox, 1988; Woelk, 1989).

The volcanic rocks have high density ~2.9 and magnetic susceptibility values with a magnetic susceptibility value of 0.002 cgs (Mariano and Hinze, 1993). The basalts additionally contain layers of normal and reverse remnant magnetization (Mariano and Hinze, 1993; Halls, 1982; Mariano and Hinze, 1993). A combination of normal and remnant magnetization causes the magnetic maxima on the total magnetic intensity and reduced to the pole magnetic maps (Figs. 24, 28).

Adjacent to the anomaly 1 on Figs. 23, 24, 25, 26, 27 and 28, gravity and magnetic minima anomalies (2, 3, 4, 5, and 6) can be found. The gravity minima (2, 3, 4, 5, and 6) have amplitudes up to -100 mGal, and magnetic minima have amplitudes up to -400 nT. Those minima anomalies are likely produced by thick sequences of less dense and magnetically less susceptible rift-related clastic sedimentary rocks that are preserved in the basins marginal to the horst (Anderson, 1992) as shown also on the geological maps (Figs. 1, 3, 10, 11). Anomaly 2 is caused by the Wellsburg Basin (WB), anomaly 3 by the Ankeny Basin (AB), anomaly 4 by the Shenandoah basin (SB), anomaly 5 by the Defiance Basin (DB), and anomaly 6 by the Duncan Basin (DC).

Between the Iowa horst basalt and the flanking sedimentary basins (Figs. 1, 3, 10, 11), there is a steep gravity gradient (Fig. 23) that indicates a high density contrast

between the basaltic volcanic rocks along the rift (anomaly 1) and the five sedimentary basins around the rift (anomalies 2, 3, 4, 5, 6) (Anderson, 1992). Although the crustal thickness changes from 52 km at the Iowa horst to 48 km southeast the horst and to 42 km northwest the horst (Moidaki et al. 2013), these crustal changes do not affect this gravity gradient as much as the basaltic-sediment density contrast.

The MCRS study area contains several additional gravity and magnetic anomalies caused by a variety Proterozoic geologic features including several intrusive rocks as dike swarms, small plutons, large cumulate bodies, diabase sills, and alkaline complexes occur in Nebraska, Iowa and Oklahoma (Lam, 1986; Woelk, 1989).

Consequently, anomalies 7, 8, and 9 (Figs. 23, 24) have both high and low gravity and magnetic values that occur surrounding the MCRS. Also, on Figs. 24 and 28 magnetic anomalies that occur within the study area (7, 8, 9, 10, and 11) have high magnetic amplitudes (200-400 nT) and low magnetic amplitudes (-300 to -400 nT).

The gravity and magnetic maxima (anomaly 7) (Figs. 23, 24, 25, 26) of more than 30 mGal and more than 350 nT respectively are likely caused by the northeast Iowa intrusive complex (NEIIC) (Drenth et al., 2015). The NEIIC is interpreted as a complex of high density mafic-ultramafic rocks and extends southeast Minnesota (Drenth et al., 2015).

Magnetic and gravity anomalies (anomaly 8) (Fig. 23, 24, 28) are interpreted to be caused by 1450 ma orogenic granitic plutons (Green Island Plutonic Belt) that intruded along a zone of weakness near the suture zone between the Mazatzal Terrane (1650 - 1620 Ma) and the Yavapai basement (1700 Ma) (Anderson, 2006).

Similarly, the gravity minima (anomaly 9) (Fig. 23) is probably caused by a large 1450 Ma felsic pluton (Spencer Pluton) (Anderson, 2006) (Fig. 11) that also contains iron-rich late stage intrusives differentiated from the cooling pluton creating the small but strongly positive magnetic anomalies in the pluton (anomaly 11, Figs. 24, 28) which is generally interpreted as consisting of Yavapai terrain ocean crust and accretionary terranes (Anderson, 2006). Magnetic anomalies 9 and 10 contain magnetic maxima and gravity lows minima, and are interpreted to be caused by felsic plutons, most of them related to a 1450 ma granite/rhyolite terrane intrusive complex (Anderson, 2006) (Fig. 11).

MODELING AND DISCUSSION

To obtain a more quantitative model of the crustal structure of the MCRS in Iowa, gravity and magnetic models were constructed along four profiles (A-A', B-B', C-C', and D-D') across the MCRS (Fig. 29). The locations of these segments were selected based on the location of the major geological features, the trend of the MCRS and the location of the gravity data. For each segment, two models were constructed to help offset the lack of constraints defining the deeper structure of the MCRS. So, to illustrate possible models that fit the observed gravity and magnetic data, the lower crustal and upper mantle structures and physical property values were varied to explore the various possible matches for each profile.

The models were derived using a two-dimensional forward modeling algorithm, where the calculated gravity and magnetic anomalies are determined using the gravity station elevation and magnetic data flight line elevations. In order to reduce the nonuniqueness of gravity and magnetic models, constraints were applied, including geological and drill hole information and results from deep and shallow seismic investigations (Wold and Hinze, 1982; Woelk and Hinze, 1991; Anderson, 2006; Shen et al., 2013). Fortunately, the MCRS has been studied extensively outside of Iowa and it is enriched with previous geological and geophysical studies (e.g., Wold and Hinze, 1982; Mariano and Hinze, 1993; Woelk and Hinze, 1991; Anderson, 1992; Shen et al., 2013; Gallegos et al., 2014) that were used as guides to constructing reasonable geological models.

There have been numerous gravity and magnetic studies outside of Iowa of the MCRS including those by Woelk and Hinze (1991), Anderson (1992), and Mariano and

Hinze (1993). These studies provide a basis for the construction of the MCRS models in Iowa. One of the most important geophysical studies along the MCRS in Iowa is Anderson (1992), who used seismic reflection data, gravity modeling and drill hole information to model the crustal structure of the MCRS in Iowa (Figs. 19, 20, and 21). In his models, he divided the crust into three zones: 1) upper crust from surface to 12.8 km, 2) middle crust from 12.8 to 23 km, and 3) lower crust from 23 to 41-50 km depths. Also, he estimated the thicknesses of the Precambrian sedimentary basins around the MCRS as shown in Fig. 10. The lower crust and upper mantle structure of each model was estimated from the seismic tomographic models determined from the 70 km spaced Earthscope broadband data (Shen et al., 2013) and receiver functions determined from broadband seismic data (Moidaki et al., 2013). These seismic models showed that the crustal thickness changes from 52 km at the Iowa horst to 48 km southeast of the rift and 42 km northwest of the rift.

Shen et al. (2013) estimated that underplated mafic material at the bottom of the lower crust may exist but the size of this material is uncertain due to the wide spacing of the seismic stations. Underplating materials were also modeled using gravity data (Hinze et. al 1991). Additionally, Woelk and Hinze (1991) showed that this mafic material formed during the rifting was not continuous from the mantle to the upper crust but occurred in lenticular blobs scattered within the lower and upper crust. The geology of the Precambrian surface in Iowa was estimated using available drill hole information (Anderson, 2006; Fig. 11). This information was useful not only to constrain the analysis of gravity and magnetic maps, but to estimate the location of the various Precambrian bodies including the granite/rhyolite terrane complex and felsic pluton (spencer pluton).

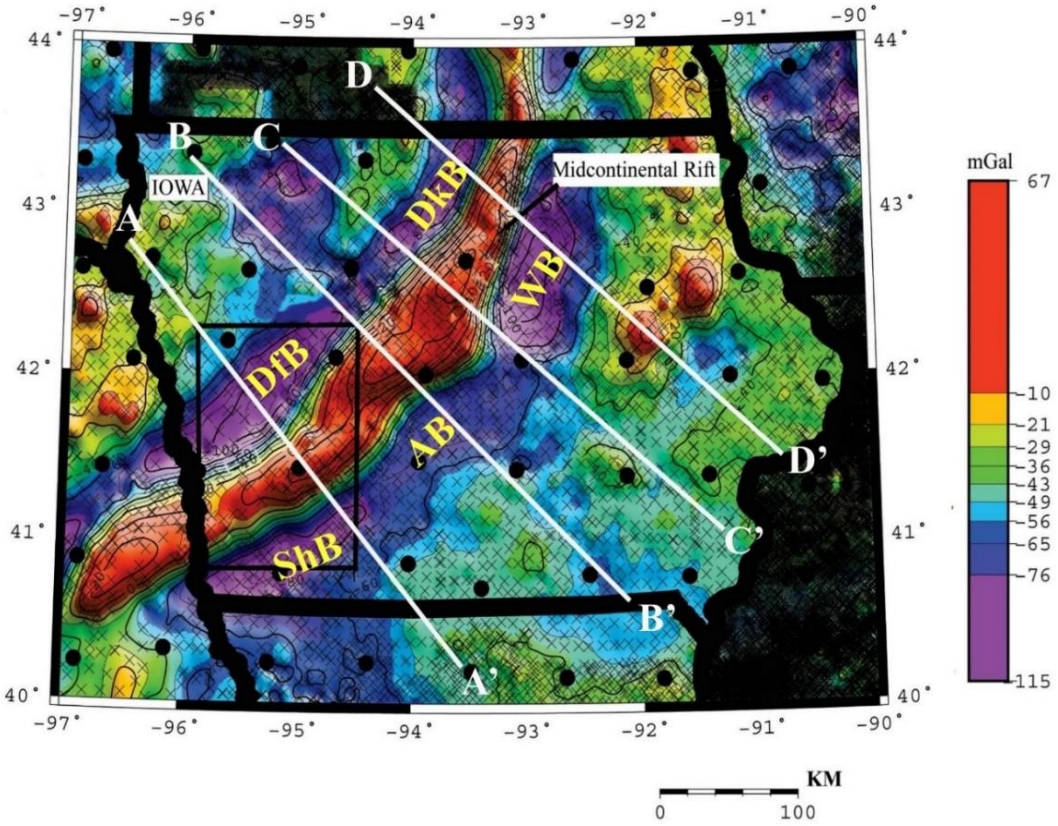

Figure 29. Bouguer gravity anomaly map of Iowa showing the locations models across the MCRS. The contour interval is 20 mGal. X-location of gravity stations. Circles-Earthscope MT stations. White lines represent the location of the four models. Yellow abbreviations are the basins; ShB (Shenandoah Basin), AB (Ankeny Basin), WB (Wellsburg Basin), DfB (Defiance Basin), DkB (Duncan Basin).

There are no density and magnetic susceptibility values available for the MCRS, nor Paleozoic sedimentary units or Precambrian lithologies in Iowa. Thus, starting values were used from previous gravity and magnetic modeling of the MCRS outside of Iowa (Woelk and Hinze 1991; Mariano and Hinze 1993) together with average magnetic values from rock samples worldwide (Telford et al., 1990). Since these values are non-unique, they were allowed to vary by 15% in the modeling process. Additionally, for the Earth's average magnetic field needed to model the magnetic data, we used an inducing field value of 55700 A/m, inclination of 70 degrees, and declination of 4.4 degrees.

Paleomagnetic studies in the northern portions of the MCRS along eastern Lake Superior (Fig. 17) have shown that there is a significant remnant magnetization component (Mariano and Hinze, 1993). The remnant magnetization components have been applied in our modeling in order to match the observed magnetic anomalies. With no paleomagnetic studies on the mafic material in the MCRS in Iowa, we used starting values reported by Mariano and Hinze (1993) for the eastern Lake Superior region. Mariano and Hinze (1993) constructed this 2D forward magnetic model in (Fig. 17) using normal remnant magnetization with inclination of 40 degree and a declination of 290 degree and a reversed remanent magnetization component with inclination of 60 degree and a declination of 110 degree. The normal remnant magnetic component is represented as basalt 1 body (Figs. 30, 31, 32, 33, 34, 35, 36, 37 and 39), the reverse remnant magnetization component is shown as basalt 2 body (Figs. 30, 31, 32, 33, 34, 35, 36, 37 and 39). The magnitude of the induced magnetization was 2.9 A/m, and the magnitude of the remnant magnetization 4.5 A/m (Mariano and Hinze, 1993). These values were also adjusted up to 15% in order to match the observed magnetic anomalies.

The uncertainty of the location and size of the underplating materials led us to construct two different models for each profile to show a range of possible models that can explain the observed anomalies. Our models were constrained by Moho depths Moidaki et al., (2013) and Shen et al. (2013), and gravity models of Anderson (1992), Behrendt et al., (1988) and Woelk and Hinze (1991). Also, we integrated the magnetic anomaly with the gravity anomaly to further constrain the models. To fit the observed gravity and magnetic anomalies outside the MCRS, various bodies, in particular the

Precambrian bodies, were positioned in the upper crust and their geometries modified until an acceptable match between the calculated and observed anomalies was obtained.

6.1. Combined Gravity and Magnetic Models Along Profile A-A'

6.1.1 Model 1. Profile A-A' (Fig. 29) extends for more than 240 km and crosses the DfB, the Iowa Horst, and then the ShB. The crust is divided into three layers upper, middle, and lower crust based on the gravity modeling of Anderson (1992). The crustal thickness underneath the MCRS ranges between 42 and52 km (Moidaki et al., 2013). The upper crust extends from the surface to 12.8 km, the middle crust from 12.8 to 23 km, and the lower crust from 23 to 41-50 km (Figs. 30 and 31). The depth of the crustal-mantle boundary has a range of 42-52 km that was constrained by seismic receiver functions (Moidaki et al., 2013) and modified to fit the observed gravity and magnetic anomalies (Figs. 30 and 31). The Phanerozoic sediments (Phs) lay on the upper part of the upper crust with thicknesses that reach up to 1.2 km depth with the initial thickness based on 1.5 km (Anderson, 1992) (Figs. 30 and 31).

A maximum Bouguer gravity anomaly value of ~50 mGal and a maximum magnetic intensity value of ~680 nT occur over above the center of the Iowa Horst (anomaly 1) (Figs. 23 and 24). The Iowa horst (MCRS basalt block) is modeled as a high density block that merges the basalt1 and basalt2 blocks, these basalt blocks have thicknesses of up to 13 km. The Iowa Horst is located within the upper crust and consists of mainly basaltic and mafic rocks (Green, 1982; Fox, 1988, and Woelk, 1992). The Iowa horst is almost 80 km wide under the Phanerozoic sediment and narrows to 20 km at the base of the upper crust (Fig. 30), with mafic intrusions occurring up to 20 km in depth

within the middle crust. Based on seismic reflection data, and gravity and magnetic modeling, Woelk and Hinze (1991) inferred lenticular mafic bodies being present within the lower crust. They implied that these mafic layers were caused by the mantle plume intrusions that originated from the upper mantle and made their way towards the crust.

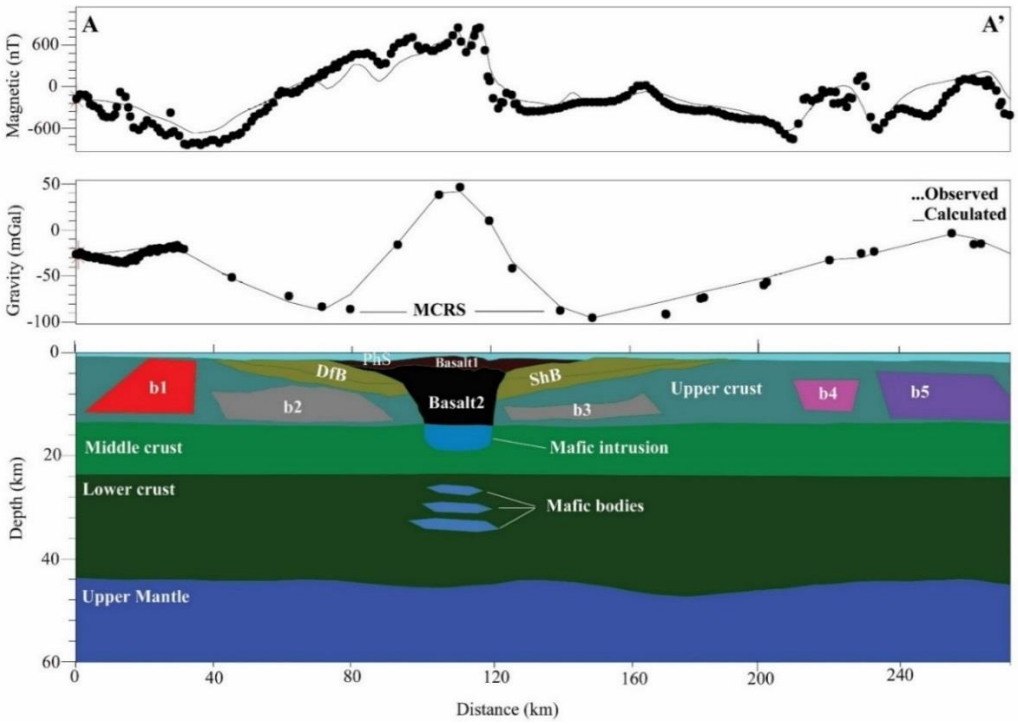

Figure 30. Integrated gravity and magnetic model along profile A-A' (Fig. 29) that emphasizes the lithospheric structure without underplating in the lower crust of the MCRS in Iowa. Densities ($_{\varrho}$) are in gm/cc and magnetic susceptibilities (k) are in emu. Phs (Phanerozoic sediments) = ($_{\varrho}$=2.5, k=0.00001). Upper crust ($_{\varrho}$=2.7, k=0.0005). Middle crust ($_{\varrho}$=2.85, k=0.0004). Lower crust ($_{\varrho}$=2.93, k=0.0003). Upper mantle ($_{\varrho}$=3.3, k=0.003). Mafic intrusion ($_{\varrho}$=2.9, k=0.0025). Mafic bodies ($_{\varrho}$=2.9, k=0.002). Basalt1 (($_{\varrho}$=2.94, k=0.002; normal remnant magnetization (remnant magnetization (r) =0.0027, Inc =40°, Dec =290°)). Basalt2 (($_{\varrho}$=2.94, k=0.002; reverse remnant magnetization (r=0.0022, Inc =60°, Dec =110°)). b1 (high gravity and low magnetic body) = ($_{\varrho}$=2.75, k=0.0001). b2 (felsic plutons) = (($_{\varrho}$=2.73, k=0.0018; normal remnant magnetization (r =0.0045, Inc =40°, Dec =290°)). b3 (felsic plutons) = (($_{\varrho}$=2.77, k=0.0014; normal remnant magnetization (r=0.0025, Inc =40°, Dec =290°)). b4 (high gravity and magnetic body) = (($_{\varrho}$=2.85, k=0.0015; normal remnant magnetization (r=0.003, Inc =40°, Dec =290°)). b5 (high gravity and magnetic body) = (($_{\varrho}$=2.9, k=0.0017; normal remnant magnetization (r=0.0025, Inc =40°, Dec =290°)). ShB (Shenandoah Basin) = ($_{\varrho}$=2.4, k=0.0001). DfB (Defiance Basin) = ($_{\varrho}$=2.4, k=0.0001).

In Iowa, the deep seismic reflection data are not available to image such layers and the Earthscope broadband seismic data do not have the resolution to image such small bodies.

On the western side of the Iowa horst, a minimum gravity anomaly values of -87 mGal occurs over the DfB (Anderson, 1988) (anomaly 5) (Figs. 23) with a thickness of 5.8 km. On the eastern side of the Iowa horst, a minimum gravity anomaly value of -93 mGal occurs over the ShB (Anderson, 1988) (anomaly 4) (Figs. 23) with a thickness of 5 km. These thicknesses roughly agree with the values imaged by seismic reflection data (Anderson, 1992). A magnetic maxima of ~240 nT (anomaly 10, Figs. 24 and 28) west of the Iowa horst and -100 nT east of the Iowa horst (anomaly 9, Fig. 24 and 28), with both anomalies correlating with gravity anomaly lows (Fig. 23). These anomalies are modeled by bodies b2 and b3, respectively (Fig. 30). Theses anomalies could be produced by felsic plutons that are probably related to the 1450 ma granite/rhyolite terrane intrusive complexes (Anderson, 2006). Block b1 represents a body with low magnetic and high gravity anomaly values, while b4 and b5 represent bodies of high gravity and magnetic anomalies.

6.1.2 Model 2. A second model (Fig. 31) was created along profile 1 that contains essentially the same upper crustal bodies but modifies the geometry of the MCRS related features due to the presence of underplated mafic material at the base of crust or a upper mantle depleted in iron rich minerals that formed during the rifting of the midcontinental (Hinze et al., 1997; Shen et al., 2013). Thinner crust or underplating is common in active continental rifts including the East African rift (Braile et al., 1994) and Rio Grande Rift

(Wilson et al., 2005). The relatively low Vs indicates less depleted material formed from upwelling mantle material that occurred during rifting (Shen et al., 2013).

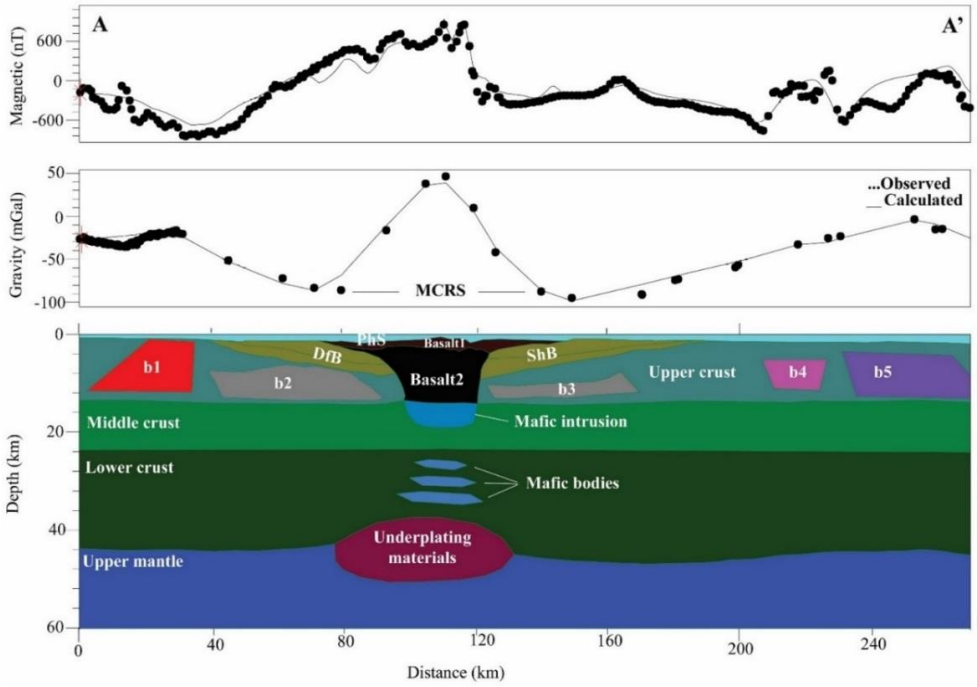

Figure 31. Integrated gravity and magnetic model along profile A-A' that shows the mantle depletion of iron-rich minerals causing the presence of underplated in the upper mantle. Densities are in gm/cc and magnetic susceptibilities are in emu. Phs (Phanerozoic sediments) = ($_{\varrho}$=2.5, k=0.00001). Upper crust ($_{\varrho}$=2.7, k=0.0005). Middle crust ($_{\varrho}$=2.85, k=0.0004). Lower crust ($_{\varrho}$=2.93, k=0.0003). Upper mantle ($_{\varrho}$=3.3, k=0.003). Basalt1 (($_{\varrho}$=2.94, k=0.002; normal remnant magnetization (r=0.0027, Inc =40°, Dec =290°)). Basalt2 (($_{\varrho}$=2.94, k=0.002; reverse remnant magnetization (r=0.0022, Inc =60°, Dec =110°)). Mafic intrusion ($_{\varrho}$=2.9, k=0.0025). Mafic bodies ($_{\varrho}$=2.9, k=0.002). Underplating materials ($_{\varrho}$=3.08, k=0.002). b1 (high gravity and low magnetic body) = ($_{\varrho}$=2.75, k=0.0001). b2 (felsic plutons) = (($_{\varrho}$=2.73, k=0.0018; normal remnant magnetization (Mag=0.0045, Inc =40°, Dec =290°)). b3 (felsic plutons) = (($_{\varrho}$=2.77, k=0.0014; normal remnant magnetization (Mag=0.0025, Inc =40°, Dec =290°)). b4 (high gravity and magnetic body) = (($_{\varrho}$=2.85, k=0.0015; normal remnant magnetization (r=0.003, Inc =40°, Dec =290°)). b5 (high gravity and magnetic body) = (($_{\varrho}$=2.9, k=0.0017; normal remnant magnetization (r=0.0025, Inc =40°, Dec =290°)). ShB (Shenandoah Basin) = ($_{\varrho}$=2.4, k=0.0001). DfB (Defiance Basin) = ($_{\varrho}$=2.4, k=0.0001).

Also, by analogy to Lake Superior region study (Hinze et al., 1997), significant amounts of mafic material from the upper mantle may have affected the mantle down to

the MCRS. This second model (Fig. 31) that contains the underplating materials satisfies the gravity data and is also used as a second model along profiles B-B', C-C' and D-D' (Figs. 33, 35 and 37).

During the modeling process, the presence of the underplated materials had no effect on the magnetic anomalies because at the depth the underplated material occurs (~40 km) is below the Curie isothermal point depth so the magnetic minerals within the lower crust and upper mantle will not contribute to observed magnetic intensity anomaly. On the other hand, the density of the underplating materials does affect the gravity anomaly (Fig. 31). This means that the underplating materials can be a significant component of the Bouguer gravity anomaly underneath the MCRS.

6.2. Combined Gravity and Magnetic Models Along Profile B-B'

6.2.1 Model 1. Profile B-B' (Fig. 29) extends for 240 km, crosses the DfB, the Iowa Horst, and then the Ankeny Basin (AB). In this model and the following models, we will not describe the models the whole models but the main differences between profile A-A' and the other three profiles B-B', C-C' D-D'. A maximum Bouguer gravity anomaly value of +70 mGal and a maximum magnetic intensity value of + 452.5 nanoteslas nT (Fig. 32) occur above the center of the Iowa Horst (anomaly 1) (Fig. 23 and 24). The Iowa horst (MCRS basalt block) is modeled as a high density block merging basalt1 and basalt2 blocks, these basalt blocks have thicknesses to up to 13.5 km. The Iowa horst has almost 100 km wide under the Phanerozoic sediments and narrows to 30 km at the base of the upper crust (Fig. 32), with mafic material occurring up to 20 km in depth within the middle crust, in addition to some mafic bodies within the lower crust.

On the west of the Iowa horst (MCRS basalt block), a minimum gravity anomaly value of -77 mGal occurs over the DfB (Anderson, 1988) (anomaly 5) (Figs. 23 and 24) with a thickness of 5.8 km. On the east of the Iowa Horst, a minimum gravity anomaly value of -80 mGal occurs over the AB (Anderson, 1988) (anomaly 3) (Figs. 23 and 24) which has a thickness 4.9 km.

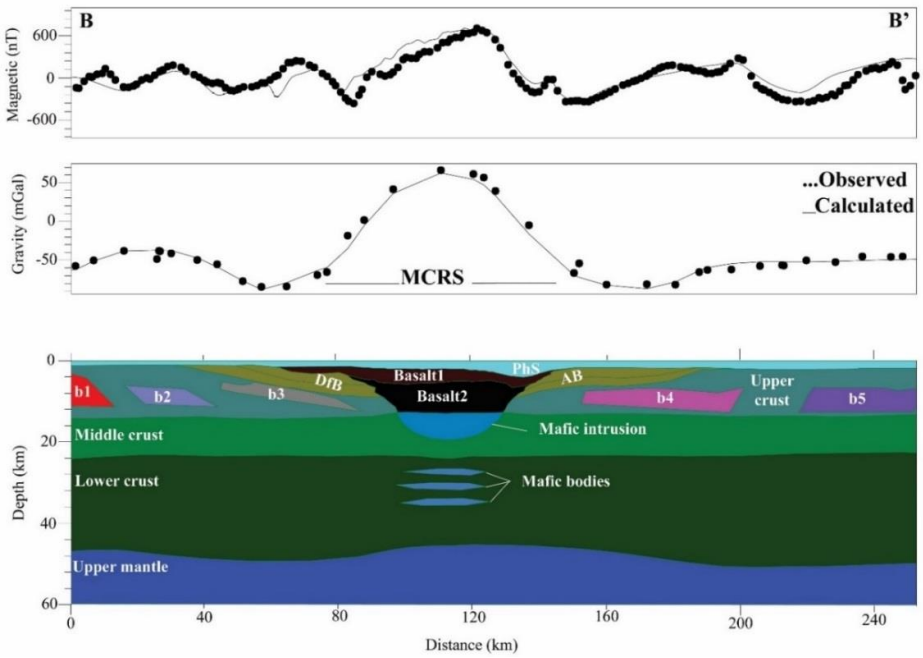

Figure 32. Integrated gravity and magnetic model along profile B-B' (Fig. 29) that emphasizes the lithospheric structure without underplating in the lower crust of the MCRS in Iowa. Densities are in gm/cc and magnetic susceptibilities are in emu. Phs (Phanerozoic sediments) = (ϱ=2.5, k=0.00001). Upper crust (ϱ=2.7, k=0.0005). Middle crust (ϱ=2.85, k=0.0004). Lower crust (ϱ=2.93, k=0.0003). Upper mantle (ϱ=3.3, k=0.003). Basalt1 ((ϱ=2.93, k=0.002; normal remnant magnetization (r=0.0024, Inc =40°, Dec =290°)). Basalt2 ((ϱ=2.94, k=0.002; reverse remnant magnetization (r=0.0022, Inc =60°, Dec =110°)). Mafic intrusion (ϱ=2.9, k=0.0025). Mafic bodies (ϱ=2.93, k=0.002). b1 (high gravity and magnetic bodies) = (ϱ=2.52, k=0.001). b2 (high gravity and magnetic bodies) = ((ϱ=2.61, k=0.0013; normal remnant magnetization (r=0.002, Inc =40°, Dec =290°)). b3 (granite/rhyolite terrane intrusive complexes) = ((ϱ=2.59, k=0.0017; normal remnant magnetization (r=0.0038, Inc =40°, Dec =290°)). b4 (large granitic pluton) = ((ϱ=2.58, k=0.0012; normal remnant magnetization (r=0.0025, Inc =40°, Dec =290°)). b5 (high gravity and magnetic bodies) = ((ϱ=2.65, k=0.0012; normal remnant magnetization (r=0.002, Inc =40°, Dec =290°)). AB (Ankeny Basin) = (ϱ=2.4, k=0.0001). DfB (Defiance Basin) = (ϱ=2.4, k=0.0001).

A high magnetic intensity value of +240 nT west of the Iowa Horst (anomaly 10) (Fig. 24) corresponds with gravity minima (Fig. 23) that is represented by the b3 body (Fig. 32). This anomaly could be due to the 1450 ma granite/rhyolite terrane intrusive complexes (Anderson, 2006). On the east of the Iowa Horst, there is a low gravity anomaly (anomaly 8) -80 mGal (Fig. 23) and a little higher magnetic intensity anomaly +200 nT. This anomaly is modeled as b4 block that might be caused by a large granitic pluton at mid-crustal level related to the shallower Green Island plutons (Anderson, 2006). Bodies b1, b2, and b5 represent bodies with high gravity and magnetic anomalies.

6.2.2 Model 2. A second model was constructed along profile 2 (Fig. 33) with essentially the same crustal bodies as model A-A' but with variations in geometry due to the effect of the underplating materials (Fig. 31). The main features are illustrated in section 6.2.1 and the underplating scenario is discussed in section 6.1.2.

6.3. Combined Gravity and Magnetic Models Along Profile C-C'

6.3.1 Model 1. Profile C-C' (Fig. 29) extends for more than 320 km, crosses the southern end of the Duncan Basin (DkB), the Iowa Horst, and then most of the way across to the southern end of the Wellsburg Basin (WB). A maximum Bouguer gravity anomaly value of +50 mGal and a maximum magnetic intensity value of + 680 nT (Fig. 34) occur over the center of the Iowa Horst (anomaly 1) (Figs. 23 and 24). The Iowa horst (MCRS basalt block) is modeled as a high density block that merges the basalt1 and basalt2 blocks, and which has a thickness up to 13 km thickness. The horst has almost 110 km wide at the Phanerozoic sediment and narrows to 30 km at the base of the upper

crust (Fig. 34), with mafic intrusions occurring up to 20 km in depth within the middle crust. In addition to some mafic bodies are within the lower crust.

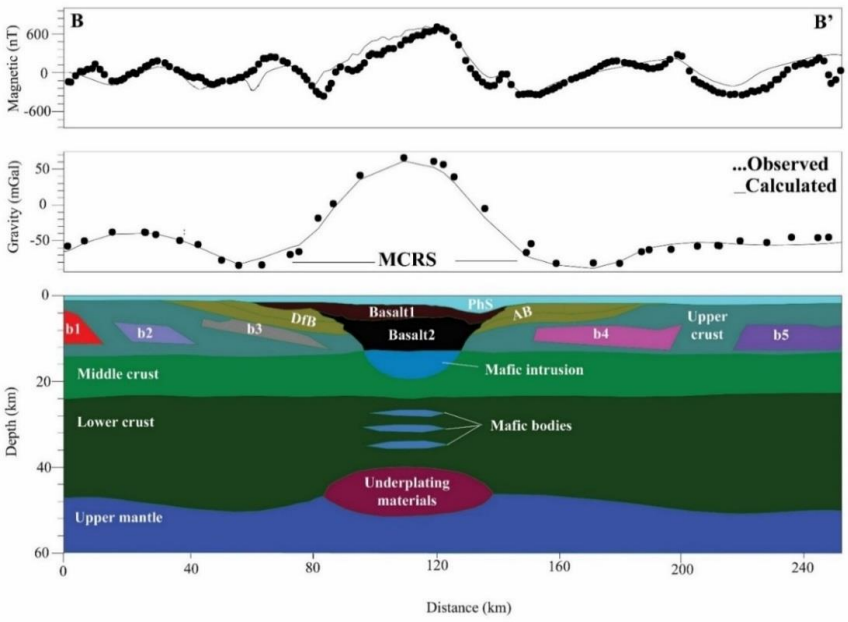

Figure 33. Integrated gravity and magnetic model along profile B-B' that shows the mantle depletion of iron-rich minerals causing the presence of underplated zone in the upper mantle. Densities are in gm/cc and magnetic susceptibilities are in emu. Phs (Phanerozoic sediments) = (ϱ=2.5, k=0.00001). Upper crust (ϱ=2.7, k=0.0005). Middle crust (ϱ=2.85, k=0.0004). Lower crust (ϱ=2.93, k=0.0003). Upper mantle (ϱ=3.3, k=0.003). Basalt1 ((ϱ=2.93, k=0.002; normal remnant magnetization (r=0.0024, Inc =40°, Dec =290°)). Basalt2 ((ϱ=2.94, k=0.002; reverse remnant magnetization (r=0.0022, Inc =60°, Dec =110°)). Mafic intrusion (ϱ=2.9, k=0.0025). Mafic bodies (ϱ=2.93, k=0.002). Underplating materials (ϱ=3.08, k=0.002). b1 (high gravity and magnetic bodies) = (ϱ=2.52, k=0.001). b2 (high gravity and magnetic bodies) = ((ϱ=2.61, k=0.0013; normal remnant magnetization (r=0.002, Inc =40°, Dec =290°)). b3 (granite/rhyolite terrane intrusive complexes) = ((ϱ=2.59, k=0.0017; normal remnant magnetization (r=0.0038, Inc =40°, Dec =290°)). b4 (large granitic pluton) = ((ϱ=2.58, k=0.0012; normal remnant magnetization (r=0.0025, Inc =40°, Dec =290°)). b5 (high gravity and magnetic bodies) = ((ϱ=2.65, k=0.0012; normal remnant magnetization (r=0.002, Inc =40°, Dec =290°)). AB (Ankeny Basin) = (ϱ=2.4, k=0.0001). DfB (Defiance Basin) = (ϱ=2.4, k=0.0001).

On the west of the Iowa horst, a minimum gravity anomaly value of -75 mGal occurs over the DkB (Anderson, 1988) (anomaly 6) (Figs. 23 and 24) with a thickness of 5.5 km. On the east of the Iowa Horst, a minimum gravity value of -70 mGal occurs over

the Wellsburg Basin (WB) (Anderson, 1988) (anomaly 2) (Figs. 23 and 24) and reaches a thickness of 4.5 km. The block b7 is necessary to adjust the lower gravity and magnetic anomalies.

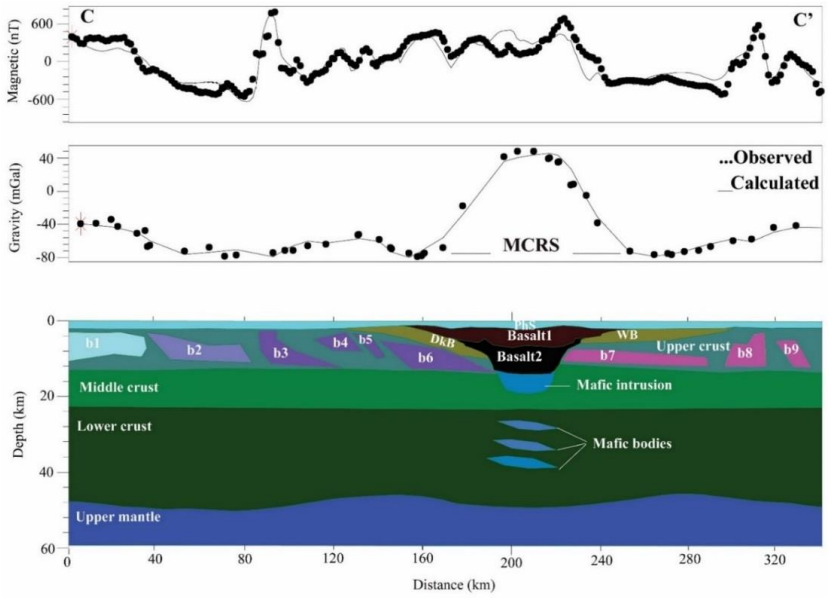

Figure 34. Integrated gravity and magnetic model along profile C-C' that emphasizes the lithospheric structure without underplating structure of the MCRS in Iowa. Densities are in gm/cc and magnetic susceptibilities are in emu. Phs (Phanerozoic sediments) = ($_{\varrho}$=2.5, k=0.00001). Upper crust ($_{\varrho}$=2.7, k=0.0005. Middle crust ($_{\varrho}$=2.85, k=0.0004). Lower crust ($_{\varrho}$=2.93, k=0.0003). Upper mantle ($_{\varrho}$=3.3, k=0.003). Basalt1 (($_{\varrho}$=2.94, k=0.002; normal remnant magnetization (Mag=0.0045, Inc =40°, Dec =290°)). Basalt2 (($_{\varrho}$=2.93, k=0.002; reverse remnant magnetization (Mag=0.0025, Inc =60°, Dec =110°)). Mafic intrusion ($_{\varrho}$=2.9, k=0.0026). Mafic bodies ($_{\varrho}$=2.9, k=0.002). b1 (low density and magnetic body) = ($_{\varrho}$=2.7, k=0.004. b2 low density and magnetic bodies = (($_{\varrho}$=2.61, k=0.0013; normal remnant magnetization (r=0.002, Inc =40°, Dec =290°)). b3 Felsic pluton (Spenser pluton) = (($_{\varrho}$=2.52, k=0.0018; normal remnant magnetization (r=0.003, Inc =40°, Dec =290°)). b4 Felsic pluton (Spenser pluton) = (($_{\varrho}$=2.5, k=0.002; normal remnant magnetization (r=0.003, Inc =40°, Dec =290°)). b5 Felsic pluton (Spenser pluton) = (($_{\varrho}$=2.8, k=0.002; normal remnant magnetization (r=0.0045, Inc =40°, Dec =290°)). b6 Felsic pluton (Spenser pluton) = (($_{\varrho}$=2.64, k=0.0019; reverse remnant magnetization (r=0.0045, Inc =60°, Dec =110°)). b7 northeast Iowa intrusive complex (NEIIC) = (($_{\varrho}$=2.7, k=0.0015; normal remnant magnetization (r=0.0025, Inc =40°, Dec =290°)). b8 (NEIIC) = (($_{\varrho}$=2.54, k=0.0018; normal remnant magnetization (r=0.0025, Inc =40°, Dec =290°)). b9 (NEIIC) = (($_{\varrho}$=2.7, k=0.0018; normal remnant magnetization (r=0.0025, Inc =40°, Dec =290°)). WB (Wellsburg Basin) = ($_{\varrho}$=2.4, k=0.0001). DkB (Duncan Basin) = ($_{\varrho}$=2.4, k=0.0001).

There are several magnetic maxima and minima west of the Iowa Horst (anomaly 11) (Fig. 24) that correspond to the gravity anomaly minima (anomaly 9) (Fig. 23). These bodies are b3, b4, b5, b6 blocks (Fig. 34). These anomalies could represent a large 1450 Ma felsic pluton called the Spenser pluton, which consists of very iron-rich late stage intrusives that may be creating small and strongly positive magnetic anomalies (Anderson, 2006) (Fig. 11). On the east of the Iowa Horst, there are a higher amplitude gravity anomalies and higher amplitude magnetic values (anomaly 7) (Figs. 23 and 24). These anomalies are modeled by including bodies b7, b8, b9 which are probably caused by NEIIC (Heitzman, 1972; Kittleson, 1975; Stepanek, 1978; Heathcote, 1979; Yaghubpur, 1979; Dixit, 1984; Sims, 1990; Anderson, 2006; Pals and Anderson, 2011). The NEIIC is interpreted as a complex of high density mafic-ultramafic rocks that extends from southeast Minnesota (Drenth et al., 2015). The origin and interpretation of these bodies are beyond the scope of this study, but they represent bodies with gravity and magnetic minima.

6.3.2 Model 2. A second model was created (Fig. 35) along profile 3 with essentially the similar crustal bodies as model 1 but with variations in geometry due to the effect of the underplating materials. The main features are discussed in section 6.3.1. The underplating materials were also discussed in section 6.1.2.

6.4. Combined Gravity and Magnetic Models Along Profile D-D’

6.4.1 Model 1. Profile D-D' (Fig. 29) extends for 320 km, crosses the northern end of the DkB, the Iowa Horst, and then most of the way across the northern end of the WB. A maximum Bouguer gravity anomaly of 25 mGal and a maximum magnetic

intensity of 635 nT (Fig. 36) occur above the center of the Iowa Horst (anomaly 1) (Figs. 23 and 24).

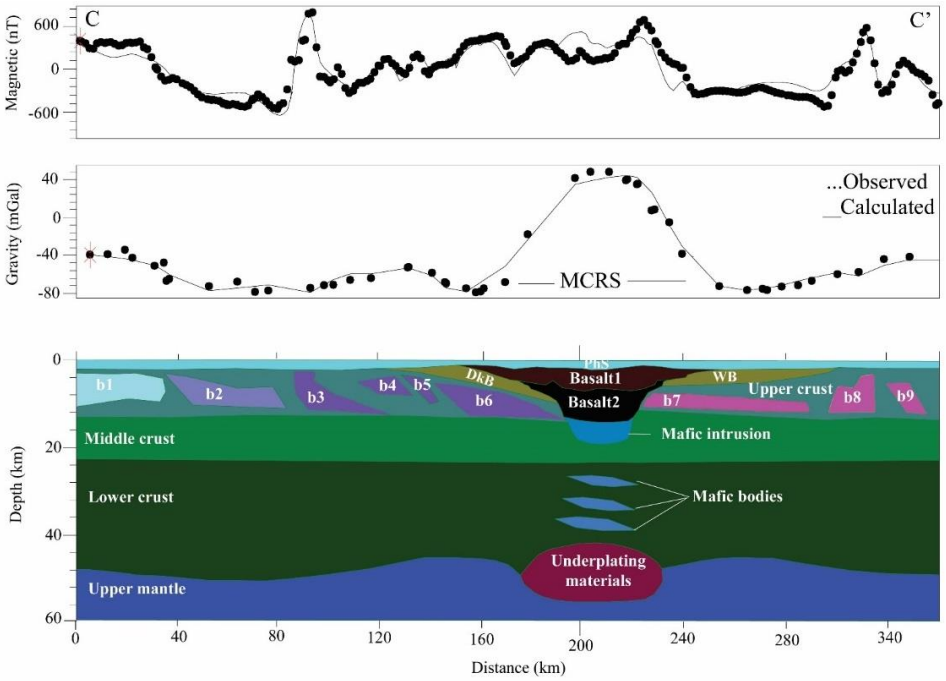

Figure 35. Integrated gravity and magnetic model along profile C-C' that shows the mantle depletion of iron-rich minerals causing the presence of underplated zone in the upper mantle. Densities are in gm/cc and magnetic susceptibilities are in emu. Phs (Phanerozoic sediments) = ($_{\varrho}$=2.5, k=0.00001). Upper crust ($_{\varrho}$=2.7, k=0.0005). Middle crust ($_{\varrho}$=2.85, k=0.0004). Lower crust ($_{\varrho}$=2.93, k=0.0003). Upper mantle ($_{\varrho}$=3.3, k=0.003). Basalt1 (($_{\varrho}$=2.94, k=0.002; normal remnant magnetization (r=0.0045, Inc =40°, Dec =290°)). Basalt2 (($_{\varrho}$=2.93, k=0.002; reverse remnant magnetization (r=0.0025, Inc =60°, Dec =110°)). Mafic intrusion ($_{\varrho}$=2.9, k=0.0026). Mafic bodies ($_{\varrho}$=2.9, k=0.002). Underplating materials ($_{\varrho}$=3.08, k=0.002). b1 (low density and magnetic bodies) = ($_{\varrho}$=2.7, k=0.004). b2 (low density and magnetic bodies) = (($_{\varrho}$=2.61, k=0.0013; normal remnant magnetization (r=0.002, Inc =40°, Dec =290°)). b3 Felsic pluton (Spenser pluton) = (($_{\varrho}$=2.52, k=0.0018; normal remnant magnetization (r=0.003, Inc =40°, Dec =290°)). b4 Felsic pluton (Spenser pluton) = (($_{\varrho}$=2.5, k=0.002; normal remnant magnetization (r=0.003, Inc =40°, Dec =290°)). b5 Felsic pluton (Spenser pluton) = (($_{\varrho}$=2.8, k=0.002; normal remnant magnetization (r=0.0045, Inc =40°, Dec =290°)). b6 Felsic pluton (Spenser pluton) = (($_{\varrho}$=2.64, k=0.0019; reverse remnant magnetization (r=0.0045, Inc =60°, Dec =110°)). b7 northeast Iowa intrusive complex (NEIIC) = (($_{\varrho}$=2.7, k=0.0015; normal remnant magnetization (r=0.0025, Inc =40°, Dec =290°)). b8 (NEIIC) = (($_{\varrho}$=2.54, k=0.0018; normal remnant magnetization (r=0.0025, Inc =40°, Dec =290°)). b9 (NEIIC) = (($_{\varrho}$=2.7, k=0.0018; normal remnant magnetization (r=0.0025, Inc =40°, Dec =290°)). WB (Wellsburg Basin) = ($_{\varrho}$=2.4, k=0.0001). DkB (Duncan Basin) = ($_{\varrho}$=2.4, k=0.0001).

The Iowa horst (MCRS basalt block) is modeled as a high density block that merges basalt1 and basalt2 blocks, with thickness of to up to 13 km. The Iowa horst is almost 80 km wide at the Phanerozoic sediment and narrows to 30 km at the base of the upper crust (Fig. 36), with mafic intrusions occurring up to 18 km in depth within the middle crust. In addition, there are mafic bodies within the lower crust.

On the west side of the Iowa horst (MCRS basalt block), a minimum gravity anomaly value of -120 mGal and a magnetic intensity value of -600 nT occur over the DkB (Anderson, 1988) (anomaly 6) (Figs. 23 and 24) with a thickness of 6.7 km. On the east side of the Iowa Horst, a minimum gravity anomaly value of -80 mGal and a magnetic intensity value of -402 nT occur over the Wellsburg Basin (WB) (Anderson, 1988) (anomaly 2) (Figs. 23 and 24) with a 4.5 km thickness.

On the east side of the Iowa Horst, there are higher amplitude gravity (-20 to -50 mGal) and high magnetic anomaly values (0, +120, and +600 nT) (anomaly 7) (Figs. 23 and 24). These anomalies were modeled by b5, b6, and b7 which might be caused by the NEIIC (Heitzman 1972, Kittleson 1975, Stepanek 1978, Heathcote 1979, Yaghubpur 1979, Dixit 1984, Sims 1990, Anderson 2006, Pals and Anderson 2011). The NEIIC is interpreted as a complex of high density mafic-ultramafic rocks southeast Minnesota (Drenth et al., 2015). West of the Iowa Horst, there are a series of magnetic maxima and minima with values of up to +800 nT above anomaly 11 (Fig. 24). These anomalies were fitted after inserting b2, b3, and b4 blocks (Fig. 34). These anomalies could be caused by Keweenawan plutonic rocks (Anderson, 2006) (Fig. 11). Block b1 represents a body with gravity and magnetic maxima anomalies.

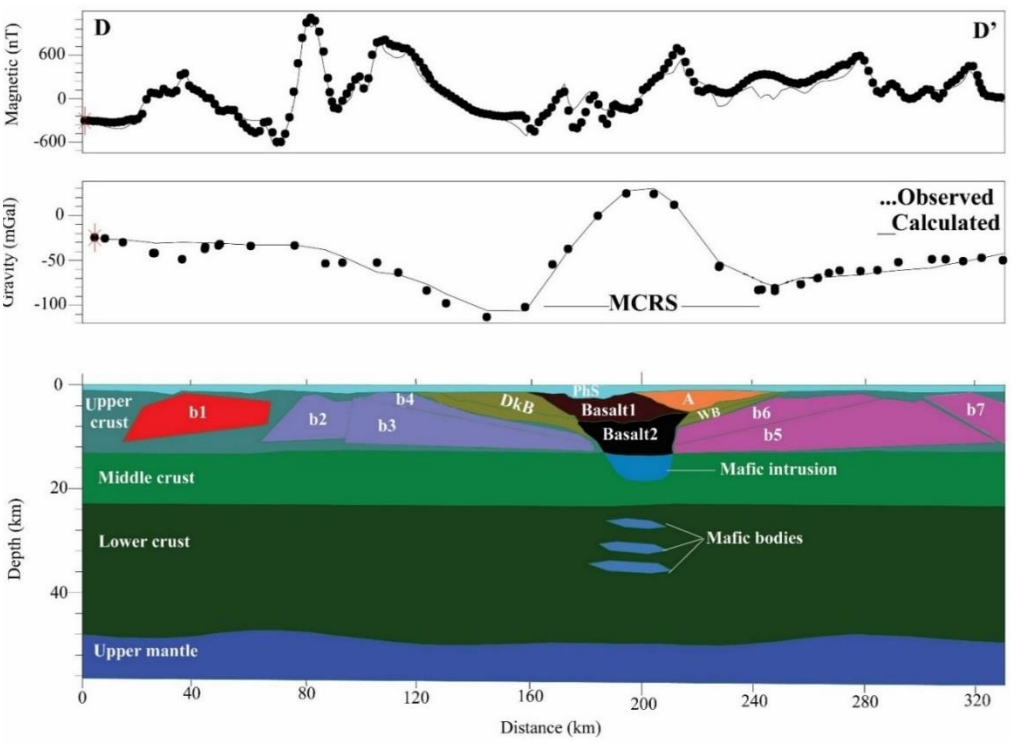

Figure 36. Integrated gravity and magnetic model along profile D-D' that emphasizes the lithospheric structure of the MCRS in Iowa. Densities are in gm/cc and magnetic susceptibilities are in emu. Phs (Phanerozoic sediments) = ($_{\varrho}$=2.5, k=0.00001). Upper - crust ($_{\varrho}$=2.7, k=0.0005). Middle crust ($_{\varrho}$=2.85, k=0.0004). Lower crust ($_{\varrho}$=2.93, k=0.0003). Upper mantle ($_{\varrho}$=3.3, k=0.003). Basalt1 (($_{\varrho}$=2.91, k=0.002; normal remnant magnetization (r=0.0024, Inc =40°, Dec =290°)). Basalt2 (($_{\varrho}$=2.92, k=0.002; reverse remnant magnetization (r=0.0021, Inc =60°, Dec =110°)). Mafic intrusion ($_{\varrho}$=2.89, k=0.0023). Mafic bodies ($_{\varrho}$=2.9, k=0.002). b1 high density and magnetic bodies = (($_{\varrho}$=2.7, k=0.0015; normal remnant magnetization (r=0.0025, Inc =40°, Dec =290°)). b2 Keweenawan plutonic rocks = (($_{\varrho}$=2.7, k=0.0034; normal remnant magnetization (r=0.0045, Inc =40°, Dec =290°). b3 Keweenawan plutonic rocks = (($_{\varrho}$=2.6, k=0.0033; normal remnant magnetization (r=0.0045, Inc =40°, Dec =290°)). b4 Keweenawan plutonic rocks = (($_{\varrho}$=2.65, k=0.0029; normal remnant magnetization (r=0.0045, Inc =40°, Dec =290°)). b5 northeast Iowa intrusive complex (NEIIC) = (($_{\varrho}$=2.59, k=0.0033; reverse remnant magnetization (r=0.0045, Inc =60°, Dec =110°)). b6 (NEIIC) = (($_{\varrho}$=2.58, k=0.0029; normal remnant r (Mag=0.0045, Inc =40°, Dec =290°)). b7 (NEIIC) = (($_{\varrho}$=2.65, k=0.0018; normal remnant magnetization (r=0.0035, Inc =40°, Dec =290°)). A (Anomalous magnetic body) = (($_{\varrho}$=2.91, k=0.0045; normal remnant magnetization (r=0.0045, Inc =40°, Dec =290°)). WB (Wellsburg Basin) = ($_{\varrho}$=2.4, k=0.0001). DkB (Duncan Basin) = ($_{\varrho}$=2.4, k=0.0001).

6.4.2 Model 2. A second model along profile 3 was constructed (Fig. 37) with essentially the same crustal bodies as Model 1 but with variations in geometry due to the

effect of the underplating materials. The main features were illustrated in section 6.4.1. and the underplating materials discussed in section 6.1.2.

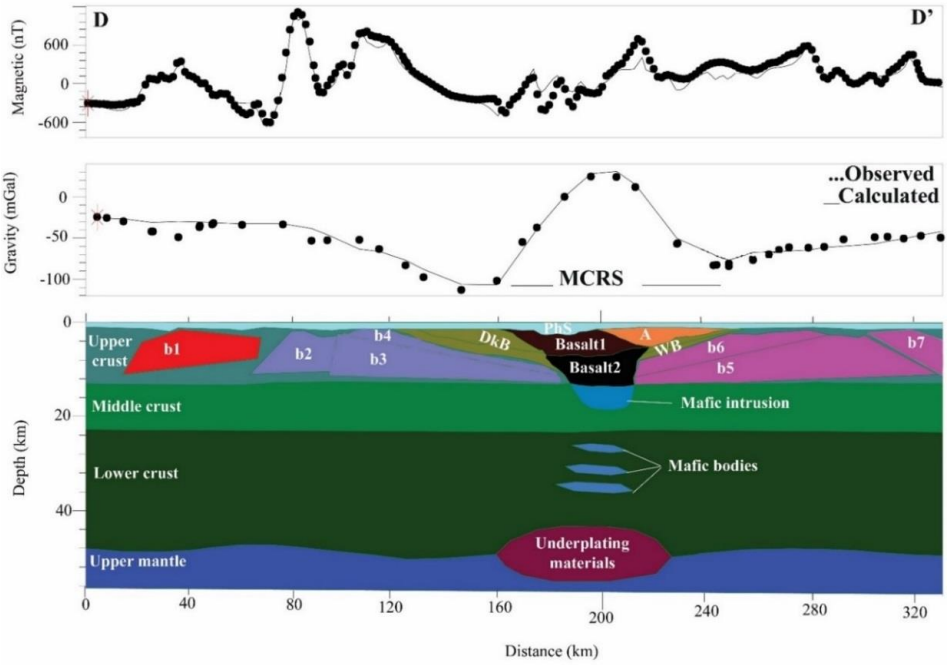

Figure 37. Integrated gravity and magnetic model along profile D-D' that shows the mantle depletion causing the presence of underplated zone on the upper mantle. Densities are in gm/cc and magnetic susceptibilities are in emu. Phs (Phanerozoic sediments) = ($_{\varrho}$=2.5, k=0.00001). Upper crust ($_{\varrho}$=2.7, k=0.0005). Middle crust ($_{\varrho}$=2.85, k=0.0004). Lower crust ($_{\varrho}$=2.93, k=0.0003). Upper mantle ($_{\varrho}$=3.3, k=0.003). Basalt1 (($_{\varrho}$=2.91, k=0.002; normal remnant magnetization (r=0.0024, Inc =40°, Dec =290°)). Basalt2 (($_{\varrho}$=2.92, k=0.002; reverse remnant magnetization (r=0.0021, Inc =60°, Dec =110°)). Mafic intrusion ($_{\varrho}$=2.89, k=0.0023). Mafic bodies ($_{\varrho}$=2.9, k=0.002). Underplating materials ($_{\varrho}$=3.08, k=0.002). b1 high density and magnetic bodies = (($_{\varrho}$=2.7, k=0.0015; normal remnant magnetization (r=0.0025, Inc =40°, Dec =290°)). b2 Keweenawan plutonic rocks = (($_{\varrho}$=2.7, k=0.0034; normal remnant magnetization (r=0.0045, Inc =40°, Dec =290°)). b3 Keweenawan plutonic rocks = (($_{\varrho}$=2.6, k=0.0033; normal remnant magnetization (r=0.0045, Inc =40°, Dec =290°)). b4 Keweenawan plutonic rocks = (($_{\varrho}$=2.65, k=0.0029; normal remnant magnetization (r=0.0045, Inc =40°, Dec =290°)). b5 northeast Iowa intrusive complex (NEIIC) = (($_{\varrho}$=2.59, k=0.0033; reverse remnant magnetization (r=0.0045, Inc =60°, Dec =110°)). b6 (NEIIC) = (($_{\varrho}$=2.58, k=0.0029; normal remnant magnetization (r=0.0045, Inc =40°, Dec =290°)). b7 (NEIIC) = (($_{\varrho}$=2.7, k=0.0018; normal remnant magnetization (r=0.0035, Inc =40°, Dec =290°)). A (Anomalous magnetic body) = (($_{\varrho}$=2.91, k=0.0045; normal remnant magnetization (r=0.0045, Inc =40°, Dec =290°)). WB (Wellsburg Basin) = ($_{\varrho}$=2.4, k=0.0001). DkB (Duncan Basin) = ($_{\varrho}$=2.4, k=0.0001).

Both models are similar in the major components to the Lake Superior gravity and magnetic models (Wold and Hinze, 1982; Behrendt et al., 1988) and to the gravity and magnetic model across the MCRS in northeastern Kansas (Woelk and Hinze, 1991). The models in this investigation have an average crustal thickness of 48 km, with an average depth to the upper basalt surface of 2 km, and an average 90 km width of the upper surface of the basalt body. The four models (Figs. 30, 31, 32, 33, 34, 35, 36, and 37) have subtle differences between them across the MCRS. The crustal thickness ranges from 48-52 km, the amount of the underplating materials for models B-B' and D-D' (Figs. 32, 33, 36, 37) is higher than for models A-A' and C-C' (Figs. 30, 31, 34, 35). Also, the volume, width and thickness of basalt for models B-B' and D-D' are higher than that of models A-A' and C-C', which are all related directly to the amount of the underplating materials in each model.

Chandler et al. (1989) and Hinze et al. (1992) interpreted critical points that are applicable to the MCRS in Minnesota, Wisconsin, and Iowa. One of these points is the presence of the deep mafic roots at the base of the volcanic rocks (basalts 1 and 2 in our models) (Figs. 30, 31, 32, 33, 34, 35, 36, and 37). These deep mafic roots are represented in our models as (mafic intrusion) (Figs. 30, 31, 32, 33, 34, 35, 36, and 37).

The presence of mafic bodies underneath volcanic rocks was suggested by Chandler et al. (1989), Anderson (1992), Hinze et al. (1992), Merino et al., (2013), and also confirmed by our models (Figs. 30, 31, 32, 33, 34, 35, 36, and 37). This confirmation of the mafic bodies suggests that the MCRS was initiated by a plume derived magma along plate boundaries.

Models 2 along profiles (Figs. 31, 33, 35, 37) are geologically more reasonable than model 1 (Figs. 30, 32, 34, 36). First, the broadband seismic study of Shen et al. (2013) suggested the presence of less depleted materials due to the slower shear wave velocity at the uppermost mantle (Fig. 14b). However, they also noted that the presence of less depleted materials has a limited effect on the shear wave velocity in the upper mantle (Shen et al., 2013), so the cause of slower velocities needed more analysis. Our gravity and magnetic models provides additional evidence for the presence of the underplated material. Second, the high volume of basaltic materials of our models (Figs. 30, 31, 32, 33, 34, 35, 36, and 37) especially model 2 (Figs. 32 and 33) represents similar results as the model 3 constructed by Merino et al., (2013). They stated that the volume of magma increases at Lake Superior and the western arm of the MCRS and decreases at the eastern arm of the rift.

The underplating materials obtain in our models agree with Shen et al. (2013) models, and the deep mafic intrusion of this study that reported by Merino et al. (2013) which strengthens the hypothesis that the MCRS was initiated as a part of an evolving plate boundary system rather than an isolated midplate volcanism (Merino et al., 2013). Consequently, this study strongly supports the presence of the underplating materials at the uppermost mantle, as suggested by previous gravity and magnetic models to the north of Iowa (Hinze et al. 1992) and seismic tomographic models (Shen et al. 2013).

To show the gravity contribution of each layer in the gravity models, a decomposition analysis was undertaken on model 2 (Fig. 33) similar to the analysis performed by Woelk (1989) in northeast Kansas. Fig. 38 showing the decomposition analysis illustrates that although a majority of the gravity maxima may have been

contributed by the basaltic material, the anomalous crustal components contribute significantly to the gravity anomaly. Of importance is that the underplated material makes a significant contribution to the final calculated gravity anomaly and its presence is considered valid.

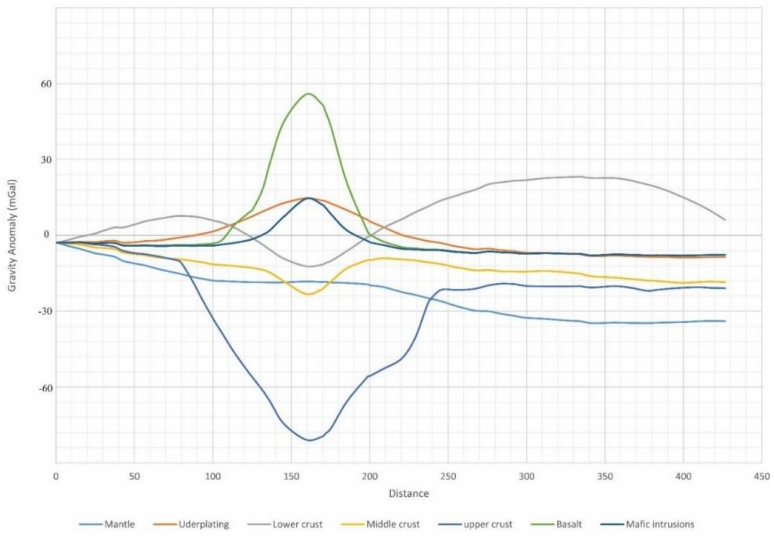

Figure 38. Decomposition of calculated gravity analysis for disturbed crust model of MCRS.

Since gravity and magnetic modeling is nonunique and two geological reasonable models were made along each profile, we conducted a sensitivity analysis for model 2 to determine the best ranges of the physical properties, as well as the geometries of the major geologic units in our models. The basalt, mafic intrusions and the underplating materials are the main units used for the sensitivity analysis. The best ranges of the physical properties are shown in Tables 2 and 3, and the values are represented on Figs. 33 and 39. Although these ranges of properties support the nonunique solution for a model, the more constraints embedded into a model produce more reasonable results that fit within an acceptable percentage of variation. This became clear after performing the

sensitivity analysis in this study. This idea is not only clear between the models of this investigation, but also the models along the different regions of the MCRS. Although there is a little variation between model 2 (Fig. 33) and model 2 (Fig. 39) as shown also in Tables 2 and 3, the main features of both models are still the same which means the consequences of sensitivity analysis does not change the results and conclusions of this investigations.

Table 2. Sensitivity analysis values for densities and geometries for basalt, mafic intrusion and underplating materials along model profile B-B'.

Blocks	Density (gm/ccm)	Geometry	
		Depth (km)	Width (km)
Basalt	2.93-2.96	Surface (1.5-3) Bottom (12.5-15)	Surface (88-95) Bottom (31-38)
Mafic intrusion	2.9-2.96	Surface (12.5-15) Bottom (19.5-20)	(25.5-30)
Underplating materials	3.08-3.15	Surface (39-40) Bottom (49.5-51)	(53-61)

Table 3. Sensitivity analysis values magnetic properties for both basalt units and mafic intrusion unit along profile B-B'

Blocks	Magnetic properties	
	Magnetic susceptibility (Cgs)	Remnant magnetization (emu/cc)
Basalt 1	0.002- 0.0018	0.0022- 0.0024
Basalt 2	0.002- 0.0017	0.0019- 0.0022
Mafic intrusion	0.0021- 0.0025	- -

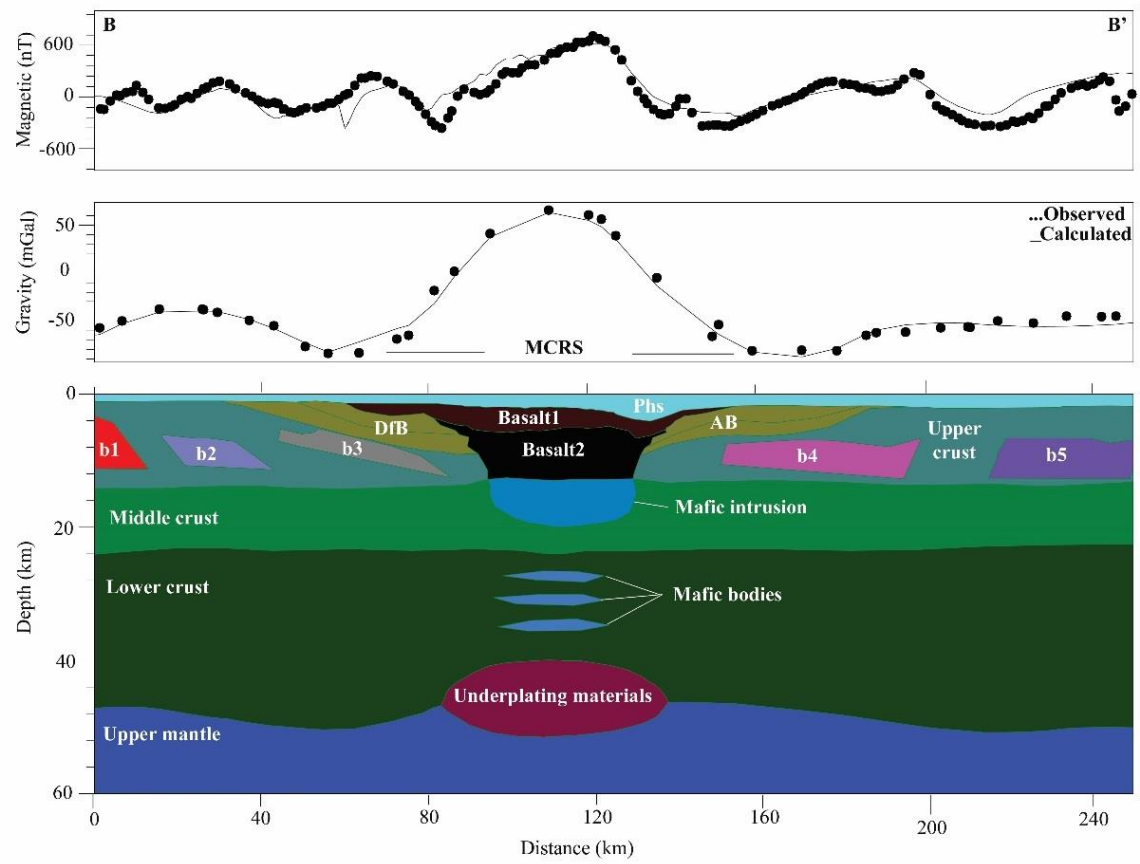

Figure 39. Integrated gravity and magnetic model along profile B-B' that shows the mantle depletion causing the presence of underplating material zone on the upper mantle. This model shows model 2 (Fig. 33) after applying the sensitivity analysis values. Densities are in gm/cc and magnetic susceptibilities are in emu. Phs (Phanerozoic sediments) = ($_{\varrho}$=2.5, k=0.00001). Upper crust ($_{\varrho}$=2.7, k=0.0005). Middle crust ($_{\varrho}$=2.85, k=0.0004). Lower crust ($_{\varrho}$=2.93, k=0.0003). Upper mantle ($_{\varrho}$=3.3, k=0.003). Basalt1 (($_{\varrho}$=2.96, k=0.0018; normal remnant magnetization (r=0.0022, Inc =40°, Dec =290°)). Basalt2 (($_{\varrho}$=2.96, k=0.0017; reverse remnant magnetization (r=0.0019, Inc =60°, Dec =110°)). Mafic intrusion ($_{\varrho}$=2.96, k=0.0023). Mafic bodies ($_{\varrho}$=2.9, k=0.002). Underplating materials ($_{\varrho}$=3.15, k=0.002). b1 high density and magnetic bodies = (($_{\varrho}$=2.7, k=0.0015; normal remnant magnetization (r=0.0025, Inc =40°, Dec =290°)). b2 Keweenawan plutonic rocks = (($_{\varrho}$=2.7, k=0.0034; normal remnant magnetization (r=0.0045, Inc =40°, Dec =290°)). b3 Keweenawan plutonic rocks = (($_{\varrho}$=2.6, k=0.0033; normal remnant magnetization (r=0.0045, Inc =40°, Dec =290°)). b4 Keweenawan plutonic rocks = (($_{\varrho}$=2.65, k=0.0029; normal remnant magnetization (r=0.0045, Inc =40°, Dec =290°)). b5 northeast Iowa intrusive complex (NEIIC) = (($_{\varrho}$=2.59, k=0.0033; reverse remnant magnetization (r=0.0045, Inc =60°, Dec =110°)). b6 (NEIIC) = (($_{\varrho}$=2.58, k=0.0029; normal remnant magnetization (r=0.0045, Inc =40°, Dec =290°)). b7 (NEIIC) = (($_{\varrho}$=2.7, k=0.0018; normal remnant magnetization (r=0.0035, Inc =40°, Dec =290°)). A (Anomalous magnetic body) = (($_{\varrho}$=2.91, k=0.0045; normal remnant magnetization (r=0.0045, Inc =40°, Dec =290°)). WB (Wellsburg Basin) = ($_{\varrho}$=2.4, k=0.0001). DkB (Duncan Basin) = ($_{\varrho}$=2.4, k=0.0001)

CONCLUSIONS

The Mid-continental rift system (MCRS) is one of the most significant tectonic features in North America. The only MCRS lithologic units exposed are those around the Lake Superior region. The lithosphere and crust has been studied geophysically by several studies using gravity, magnetic, and seismic data since the middle 1940's with the gravity and magnetic anomaly maps clearly outlining the MCRS from the Lake Superior region to northern Oklahoma by a large amplitude gravity maximum. Even though there have been geophysical studies all along the MCRS, the section within Iowa has not been studied in detailed to date and we used available gravity and magnetic data to analyze the lithospheric structure in Iowa.

Bouguer gravity, total-field magnetic intensity maps, and transformed maps including using low-pass, high-pass and band-pass filters were constructed to analyze the gravity and magnetic data associated with the MCRS and the surrounding area. On all the constructed gravity and magnetic anomaly maps, a variety of regions produced significant anomalies including the basalt within the Iowa horst, the rift related basins, the northeast Iowa intrusive complex (NEIIC), and the 1450 Ma Spenser pluton.

In order to study the lithospheric structure in more detail, four gravity and magnetic models were constructed constrained by basement drill holes, seismic reflection profiles and broadband seismic models. These integrated gravity and magnetic models fitted the observed gravity anomalies to bodies of specific densities and magnetic susceptibilities until a good fit was obtained. The models show that gravity and magnetic maxima are caused mainly by the mafic igneous rocks filling the rift and the Proterozoic

plutonic rocks including the NEIIC and the Spenser pluton, whereas the rift related basins are related to gravity and magnetic minima due to clastic sediments. The average thickness of the basalts blocks filling the MCRS is 13 km. The rift related basins have different thicknesses, DfB has 5.8 km, ShB has 5 km, AB has 4.9 km, DkB has 6.1 km, and WB has 4.5 km. This study confirms the presence of anomalous bodies that were suggested and interpreted by Woelk and Hinze (1991) to be mafic bodies (Figs. 30, 31, 32, 33, 34, 35, 36, and 37) within the lower crust.

Two models for each profile due to the nonuniquess of gravity and magnetic modeling were constructed to determine if underplating materials in the lower crust is a reasonable model in Iowa as imaged using broadband seismology (Shen et el., 2013) that suggested the presence of less depleted materials. The second model which contains the underplated materials producing a reasonable model and compares favorably to other gravity and magnetic models along the MCRS and is the preferred model for the MCRS in Iowa. In both models, the deep mafic intrusions beneath the volcanic rocks are investigated and confirmed by this study.

REFERENCES

Allenby, R. J., and Schnetzler, C. C., 1983, United States crustal thickness: Tectonophysics, v. 93, p. 13-31.

Anderson, R. R., 1992, The midcontinent rift of Iowa [PhD. thesis]: University of Iowa, 306 p.

Anderson, R. R., 2006, Geology of the Precambrian Surface of Iowa and surrounding area, Iowa Geological Survey, Open-File Map OFM-06-7.

Baker, B. N., Morgan, P., 1981, Continental rifting: progress and outlook: Eos, Transaction American Geophysical union, v. 62, p. 585-586.

Bankey, V. A., Cuevas, D., Daniels, A. A., Finn, I., 2002, Hernandez and Project Members, Digital Data Grids for the Magnetic Anomaly Map of North America, USGS, Open-File Report 02-414.

Behrendt, J. C., Green, A. G., Cannon, W. F., Hutchinson, D. R., Lee, M., Milkereit, B., Agena, W. F., and Spencer, C., 1988, Crustal structure of the Midcontinent rift system: Results from GLIMPCE deep seismic reflection profiles: Geology, v. 16, p. 81-85.

Bickford, M. E., Van Schmus, W. R., and Zietz, I., 1986, Proterozoic history of the midcontinent region of North America: Geology, v. 14, p. 492-496.

Blakely, R., and Simpson, R., 1986, Approximating edges of sources bodies from magnetic or gravity anomalies: Geophysics, v. 51, p. 1494-1498.

Braile, L. W., Wang, B., Daudt, C. R., Keller, G. R., and Patel, J. P. l., 1994, Modelling the 2-D seismic velocity structure across the Kenya rift: Tectonophysics, v. 236, p. 217-249.

Cambray, F.W., and Fujita, K., 1991, Collision induced ripoffs, ancient and modern: The Midcontinent Rift System and the Red Sea - Gulf of Aden compared (abstract). Thirty-Seventh Institute on Lake Superior Geology, Proceedings: Part 1, p. 15-16.

Chandler, V. W., McSwiggen, P. L., Morey, G. B., Hinze, W. J., and Anderson, R. R., 1989, Interpretation of seismic reflection, gravity, and magnetic data across the Middle Proterozoic Midcontinent rift system, northwestern Wisconsin, eastern Minnesota, and central Iowa: American Association of Petroleum Geologists Bulletin, v. 73, p. 261-275.

Cohen, T. J., 1966, Explosion seismic studies of the Mid-Continent Gravity High, [PhD thesis]: Madison, University of Wisconsin, 329 p.

Craddock, C., Thiel, E. C., and Gross, B., 1963, A gravity investigation of the Precambrian of southeastern Minnesota and western Wisconsin: Journal of Geophysical Research, v. 68, p. 6015-6032.

Donaldson, J. A., and Irving, E., 1972, Grenville Front and rifting of the Canadian Shield: Nature (London), Physical Science, v. 237, p. 139-140.

Drenth, B. J., Anderson, R. R., Schulz, K. J., Feinberg, J. M., Chandler, V. W., and Cannon, W. F., 2015, What lies beneath: geophysical mapping of a concealed Precambrian intrusive complex along the Iowa–Minnesota border: Canadian Journal of Earth Science, v. 52, p. 1-15.

Fox, AJ. 1988, an integrated geophysical study of the southeastern extension of the Midcontinent rift system [MS. Thesis]: West Lafayette, Indiana, Purdue University, 112 p.

Franklin, H. M., McIlwaine, W. H., Poulsen, K. H., and Wanless, R. K., 1980, Stratigraphy and depositional setting of the Sibley Group, Thunder Bay, Ontario, Canada: Canadian Journal of Earth Sciences, v. 17, p. 633-651.

Gallegos, A., Ranasinghe, N., Ni, J., and Sandvol, E., 2014, Lg attenuation in the central and eastern United States as revealed by the EarthScope Transportable Array: Earth and Planetary Science Letters, v. 402, p. 187-196.

Gordon, M. B., and Hempton, M. R., 1986, Collision-induced rifting: The Grenville Orogeny and the Keweenawan Rift of North America: Tectonophysics, v. 127, p. 1-25.

Green, J. C, 1982, Geology of Keweenaw an extrusive rocks: Geological Society of America Memoirs, v.156, p. 47-56.

Green, J. C., 1989, Physical volcanology of mid-Proterozoic plateau lavas: The Keweenawan North Shore Volcanic Group, Minnesota: Geological Society of America Bulletin, v. 101, p. 486-500.

Halls, H. 1978, the late Precambrian central North America rift system-a survey of recent geological and geophysical investigations, *in* Tectonics and Geophysics of Continental Rifts: NATO Advanced Study Institute, Series C, Mathematical and Physical Sciences, edited by Neumann, E. R., and Ramberg, I., v. 37, p. 111–123, Reidel, Dordrecht, NL. Springer Netherlands.

Halls, H. C., 1982, Crustal thickness in the Lake Superior region in geology and tectonic of the Lake Superior: Geological Society of America, Memoir, v. 156, p. 239-277.

Heathcote, S. H., 1979, Geologic interpretation of the Manchester Geophysical Anomaly, Delaware County, Iowa [MS thesis]: University of Iowa, 150 p.

Hildreth, W., 1981, Gradients in silicic magma chambers: implications for lithospheric magmatism: Journal of Geophysics Research, v. 86, p. 10153-10192.

Hinze, W. J., and Kelly, W. C., 1988, Scientific Drilling Into the Midcontinent Rift System. Eos, Transactions American Geophysical Union, v. 69, p. 1656-1657.

Hinze, W. J., Braile, L.W., and Chandler, V. W., 1990, A geophysical profile of the southern margin of the Midcontinent rift system in western Lake Superior: Tectonics, v. 9, p. 303-310.

Hinze, W., Allen, D., Fox, A., Sunwood, D., Woelk, T., and Green, A., 1992, Geophysical investigations and crustal structure of the north America Midcontinent Rift system: Tectonophysics, v. 213, p. 17-32.

Hinze, W. J., Allen, D. J., Braile, L. W., and Mariano, J., 1997, The Midcontinent rift system: A major Proterozoic continental rift: Geological Society of America Special Paper 312, p. 7-34.

Hutchinson, D. R., White, R. S., W. F., and Schulz, K. J., 1990, Keweenaw hot spot: Geophysical evidence for a 1.1 Ga mantle plume beneath the Midcontinent Rift system: Journal of Geophysical Research: Solid Earth, v. 95, p. 10869-10884.

Keller, G. R., Lidiak, E.G., Hinze, W. J., and Braile, L. W., 1983, The role of rifting in the tectonic development of the Midcontinent, USA: Tectonophysics, v. 94, p. 391-412.

Lam, C., 1986, Interpretation of state-wide gravity survey of Kansas [PhD. Thesis]: University of Kansas, 213 p.

Le Cheminant, A. N., and Heaman, L. M., 1990, Mackenzie igneous events, Canada: Middle Proterozoic hotspot magmatism associated with an ocean opening: Earth and Planetary Science Letters, v. 96, p. 38-48.

Lidiak, E. G., and Zietz, I., 1976, Interpretation of aeromagnetic anomalies between latitudes 37 degrees N and 38 degrees N in the eastern and central United States: Geological Society of America, Special Papers, v. 167, p. 1-38.

Lyons, P. L., 1950, A gravity map of the United States: Tulsa Geological Society Digest, v. 18, p. 33-43.

Mariano, J., and Hinze, W., 1993, Gravity and magnetic models of the Midcontinent rift system in eastern Lake Superior: Canadian Journal of Earth Science, v. 31, p. 661-674.

Merino, M., Keller, G. R., Stein, S., and Stein, C., 2013, Variations in Mid-Continent Rift magma volumes consistent with microplate evolution: Geophysical Research Letters, v. 40, p. 1513-1516.

Mickus, K., and Montana, C., 1999, Crustal structure of northeastern Mexico revealed through the analysis of gravity data: Geological society of America Special Paper 340 p. 357-372.

Moidaki, M., Stephen S. Gao., Liu. K, H., and Atekwana, E., 2013, crustal thickness and upper Moho sharpness beneath the midcontinent rift from receiver functions: Research in Geophysics, v. 3, p. 1-7.

Mooney, H. M., Craddock, C., Farnham, P. R., Johnson, S. H., and Volz, G., 1970, Refraction seismic investigations of the northern midcontinent gravity high: Journal of Geophysical Research, v. 75, p. 5056-5086.

Morelli, C., 1976, Modern standards for gravity surveys: Geophysics, v. 41, p. 199-199.

Morey, G. B., and Sims, P. K., 1976, Boundary between two Precambrian terranes in Minnesota and its geological significance: Geological Society of America Bulletin, v. 87, p. 141-152.

Nyquist, J. E., and Wang, H. F., 1988, Flexural modeling of the Midcontinent rift: Journal of Geophysical Research, v. 93, p. 8852-8868.

Ocola, L.C., and Meyer, R. P., 1973, Central North American Rift System: 1. Structure of the axial zone from seismic and gravimetric data: Journal of Geophysical Research, v. 78, p. 5173-5194.

Peeples. W. J., Coultrip, R. L., and Keller. G. R., 1986, Quasi-ideal spatial filters for large maps: Annuale Geophysicae, v. 4. p. 547-554

Philips, J. D., Duval, J. S., and Ambrozial, R. A., 1993, National Geophysical data grids: Gamma ray, gravity, magnetic and topographic data for the conterminous United States, U.S. Geological Survey Digital Data Series DDS-9, CD-ROM.

Skeels, D. C., 1967, What is residual gravity? : Geophysics, v. 32, p. 872-876.

Serpa, L., Setzer, T., Farmer, H., Brown, L., Oliver, J., Kaufman, S, Sharp, J., and Steeples, D. W., 1984, Structure of the southern Keweenaw rift from COCORP surveys across the Midcontinent geophysical anomaly in northeastern Kansas: Tectonics, v. 3, p. 367-384.

Shen, W., Ritzwoller, M. H., and Schulte-Pelkum, V., 2013, Crustal and uppermost mantle structure in the central U.S. encompassing the Midcontinent Rift: Journal of Geophysical Research, v. 118, p. 4325-4344.

Stein, C. A., Kely, J., Stein, S., Hindle, D., and Keller, G, R., 2015, North America's Midcontinent Rift: When rift met LIP: Geosphere, v.11, p. 1607-1616.

Tapponnier, P., and Molnar, P., 1976, Slip-line field theory and large scale continental tectonics: Nature, v. 264, p. 319-324.

Tapponnier, P., Peltzer, G., Ledain, A. Y., Armijo, R., Cobbold, P., 1982, Propagating extrusion tectonics in Asia: new insights from simple experiments with plasticine: Geology, v. 10, p. 611-616.

Telford, W. M., Geldart, L. P., and Sheriff, R. E., 1990, Applied Geophysics: Cambridge, New York, Cambridge University Press, 770 p.

Ulrych, T. J., 1968, Effect of wavelength filtering on the shape of the residual anomaly: Geophysics, v. 33, p. 15-18.

Van Schmus, W. R. and Hinze, W. J., 1985, the Midcontinent Rift System: Annual Review of Earth and Planetary Sciences, v. 13, p. 345-383.

Van Schmus, W. R., Bickford, M. E., Zietz, I., 1987, Early and Middle Proterozoic provinces in the central United States, *in* Proterozoic Lithospheric Evolution, Kroner, A., ed.: American Geophysical Union Geodynamic Series, v. 17, p. 43-68.

Verduzco, B., Fairhead, J. D., Green, C. M., and MacKenzie, C., 2004, New insights into magnetic derivatives for structural mapping: The Leading Edge, v. 23, p. 116-119.

Vervoort J.D. and Green. J.C., 1997, Origin of evolved magmas in the Midcontinent rift system, northeast Minnesota: Nd-isotope evidence for melting of Archean crust: Canadian Journal of Earth Sciences, v. 34, p. 521-535.

Vervoort, J. D., Wirth, K., Kennedy, B., Sandland, T., and Harpp, K. S., 2007, The magmatic evolution of the Midcontinent rift: New geochronologic and geochemical evidence from felsic magmatism: Precambrian Research, v. 157, p.235-268

White, R. S., 1997, Mantle temperature and lithospheric thinning beneath the Midcontinent rift system: Evidence from magmatism and subsidence: Canadian Journal of Earth Science, v. 34, p. 464-475.

Whitmeyer, S. J., and Karlstrom, K. E., 2007, Tectonic model for the Proterozoic growth of North America: Geosphere, v. 3, p. 220-259.

Wilson, D., Aster, R., West, M., Ni, J., Grand, S., Gao, W., Baldridge, W. S., Semken, S., and Patel, P., 2005, Lithospheric structure of the Rio Grande rift: Nature, v. 433, p. 851-854.

Windley, B. F., 1989, Anorogenic magmatism and the Grenville Orogeny: Canadian Journal of Earth Sciences, v. 26, p. 179-189.

Woelk, T., 1989, an integrated geophysical study of the Midcontinent Rift System in Northeastern Kansas [PhD. thesis]: Purdue University, 75 p.

Woelk, T. S., and Hinze, W. J., 1991, Model of the midcontinent rift system in northwestern Kansas: Geology, v. 19, p. 277-280.

Wold, R. J., and W, J. Hinze, eds., 1982, Geology and tectonic of the Lake Superior Basin: Geological Society of America, Memoir, 156, p. 280.

Woollard, G. P., 1943, Transcontinental gravitational and magnetic profile of North America and its relation to geologic structures: Geological Society of America Bulletin, v. 54, p. 747-789.

Zhu, T., and Brown, L. D., 1986, Consortium for Continental Reflection Profiling Michigan Survey: Reprocessing and results: Journal of Geophysical Research, v. 91, p. 11477-11495.